DISSERTATION FOR THE DEGREE OF DOCTOR OF PHILOSOPHY (PHD)

The role of osteopontin expression during malignant melanoma progression

by Tímea Kiss

UNIVERSITY OF DEBRECEN

DOCTORAL SCHOOL OF HEALTH SCIENCES

DEBRECEN, 2023

DISSERTATION FOR THE DEGREE OF DOCTOR OF PHILOSOPHY (PHD)

The role of osteopontin expression during malignant melanoma progression

by Tímea Kiss

Supervisor: Margit Balázs, PhD, DSc

UNIVERSITY OF DEBRECEN

DOCTORAL SCHOOL OF HEALTH SCIENCES

DEBRECEN, 2023

Table of contents

Abbreviations

6H5MI2C: 6-hydroxy-5-methoxyindole-2-carboxylic acid

AFP: alpha-fetoprotein

AKT: v-akt murine thymoma viral oncogene homolog

ANGPT1: angiopoietin-1

ANO9: anoctamin 9

ATCC: American Type Culture Collection

Bcl-2: B-cell lymphoma 2

BIRC5: surviving

BRAF: v-raf murine sarcoma viral oncogene homolog B1

CA9: carbonic anhydrase IX

CCL2: C-C motif chemokine 2

CDH5: VE-cadherin

CDK4: cyclin-dependent kinase 4

CDKN1B: cyclin-dependent kinase inhibitor 1B/p27

CDKN2A: cyclin-dependent kinase inhibitor 2A

CEACAM: carcinoembryonic antigen-related cell adhesion molecule 1

CI: confidence interval

Cox-2: cyclooxygenase-2

CTCs: circulating tumour cells

ctDNA: circulating tumour DNA

CTLA-4: cytotoxic T-lymphocyte-associated protein 4

CTPs: circulating tumour products

CTSB: cathepsin B

CTSD: cathepsin D

CTSS: cathepsin S

CXCL8: interleukin-8

CYT-MAA: cytoplasmic melanoma-associated antigen

DTIC: dacarbazine

ECP: eosinophil cationic protein

EGFR: epidermal growth factor receptor

EIF1B: eukaryotic translation initiation factor 1B

ENG: endoglin

ERBB2: receptor tyrosine-protein kinase erbB-2

ERBB3: receptor tyrosine-protein kinase erbB-3

FBS: fetal bovine serum

FDA: Food and Drug Administration

FFPE: formalin-fixed paraffin-embedded

FGF2: basic fibroblast growth factor

FOX01: forkhead box protein O1

GAPDH: glyceraldehyde-3-phosphate dehydrogenase

GEP: gene expression profile

GRN: progranulin

H&E: haematoxylin-eosin

HGF: hepatocyte growth factor

HIF-1α: hypoxia-inducible factor 1-alpha

HMOX1: heme oxygenase 1

HR: hazard ratio

HRP: horseradish peroxidase

IARC: International Agency for Research on Cancer

ICAM1: intercellular adhesion molecule 1

IDO: indoleamine 2,3-dioxygenase

Ig G: immunoglobulin G

IHC: immunohistochemistry

IL-2: interleukin-2

IL-6: interleukin-6

IL-8: interleukin-8

KRT6B: Keratin 6B

KRAS: kirsten rat sarcoma virus

LDH: serum lactate dehydrogenase

L-DOPA: L-3,4-dihydroxyphenylalanine

LGALS3: galectin-3

lncRNAs: long noncoding RNAs

MAGE: melanoma-associated antigen-1

MAPK: mitogen-activated protein kinase

MART-1: melanoma antigen recognized by T-cells 1

MC1R: melanocortin 1 receptor

MEK: mitogen-activated protein kinase kinase

MIA: melanoma inhibitory activity

miRNA: microRNA

MITF: microphthalmia-associated transcription factor

MMP: matrix metalloproteinase

MMP3: matrix metalloproteinase-3

mRNA: messenger RNA

MSH: melanocyte-stimulating hormones

MYC: MYC proto-oncogene

NC: negative control

NF-κB: nuclear factor kappa-light-chain-enhancer of activated B cells

NM: nodular melanoma

NRAS: neuroblastoma RAS viral (v-ras) oncogene homolog

NSCLC: non-small cell lung cancer

OPN/SPP1: osteopontin/secreted phosphoprotein 1

OS: overall survival

PBS: phosphate-buffered saline

PDGFA: platelet-derived growth factor AA

PI3K: phosphatidylinositol-4,5-bisphosphate 3-kinase

PKA: protein kinase A

PTEN: phosphatase and tensin homolog

qRT-PCR: quantitative reverse-transcription polymerase chain reaction

RAF: rapidly accelerated fibrosarcoma

RGP: radial growth phase

RIPA: radio-immunoprecipitation assay

RISC: RNA-induced silencing complex

RNAi: RNA interference

RT: room temperature

S100B: S100 calcium-binding protein B

SD: standard deviation

sICAM: soluble intercellular adhesion molecule 1

siRNA: small interfering RNA

SNAI1: snail

SPARC: secreted protein acidic and rich in cysteine

SSM: superficial spreading melanoma

STRING: Search Tool for the Retrieval of Interacting Genes

sVCAM: soluble vascular cell adhesion molecule 1

TA90: tumour-associated antigen 90

TMA: tissue microarray

TNC: tenascin C

TNM: tumour-lymph node-metastasis

TP53: cellular tumour antigen p53

UV: ultraviolet

UVA and UVB: ultraviolet - A and - B

VEGF: vascular endothelial growth factor

VGP: vertical growth phase

VIM: vimentin

WNT: wingless-type MMTV (mouse mammary tumour virus) integration site family

WST-1: water soluble tetrazolium (salt) - 1

WT: wild type

XP: xeroderma pigmentosum

YKL-40: heparin- and chitin-binding lectin YKL-40

Introduction

Melanoma is one of the most malignant forms of cancers and represents a significant public health problem globally, with several histopathological subtypes and varying incidence rates among different populations [1-3]. The incidence of melanoma varies among different populations, primarily due to genetic factors and levels of sun exposure. The incidence of the disease has been steadily increasing worldwide over the past decades, particularly among light-skinned populations. In 2020, the International Agency for Research on Cancer (IARC) estimated that there were 324,635 cases of melanomas worldwide resulting in 57,043 deaths (**Figure 1, 2**). Among these cases, 173,844 occurred in men, while 150,791 occurred in women [4].

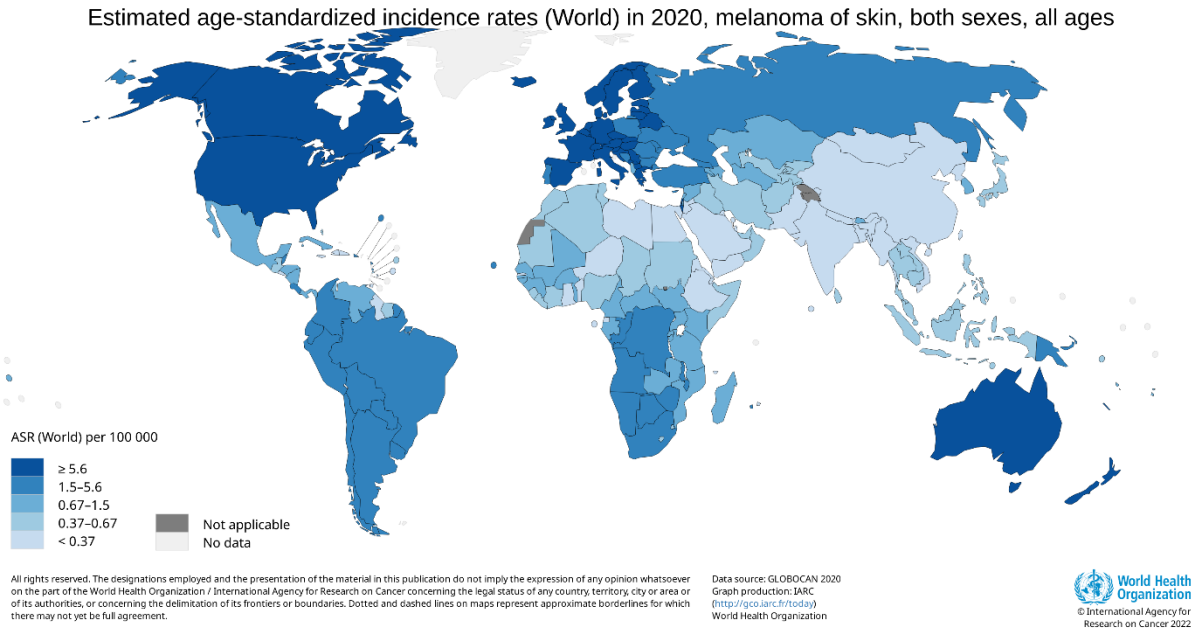

Figure 1. The estimated age-standardized incidence rate of melanoma of the skin globally. *Source: https://gco.iarc.fr/today [4].*

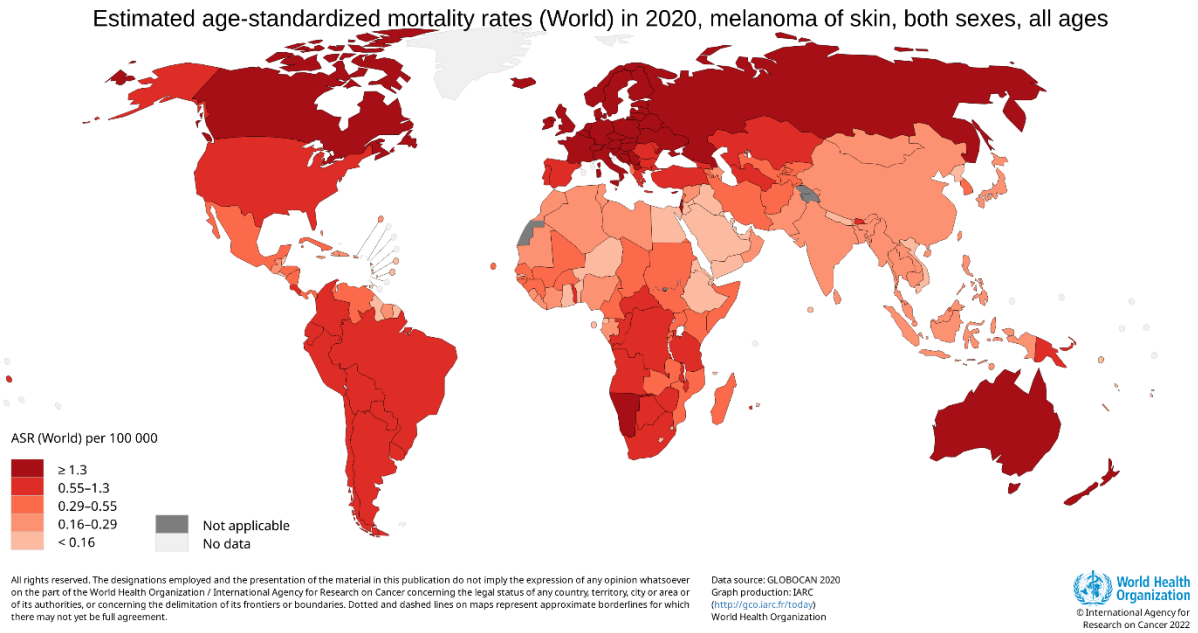

Figure 2. The estimated age-standardized mortality rate of melanoma of the skin globally.
Source: https://gco.iarc.fr/today [4].

The age-standardized incidence rates (cases/100,000 residents) of melanoma vary widely across different regions. The highest rates of melanoma incidence, estimated at 35.8 cases per 100,000 residents, as well as mortality rates 2.7 cases per 100,000 residents observed in Australia and New Zealand. In Hungary, according to GLOBOCAN data for 2020, the estimated age-standardized incidence rate was 11.4/100,000 population, while the mortality was 1.6/100,000 population [4, 5].

The development of melanoma is multifactorial, resulting from the interaction of genetic predisposition and environmental influences. Environmental factors can be divided into two categories which can be classified as exogenous and endogenous. Exogenous factors include ultraviolet radiation and the number of sunburns suffered during life. Ultraviolet (UV) radiation is a significant contributing factor in the development of the most common subtypes melanoma. Both ultraviolet-A (UVA) and ultraviolet-B (UVB) radiation are responsible for the

development of skin tumours. Radiation-induced DNA damage leads to the production of pyrimidine dimer and photoproducts that contribute to the development of melanoma. Acute sun exposure, particularly the multiple sunburn in childhood, plays a crucial role in most melanoma tumours. Epidemiological studies show that if the number of sunburns in a lifetime exceeds five, the risk for melanoma increases significantly [6, 7]. Endogenous factors include genetic variations underlying the development and progression of melanoma.

During the last decade, number of high-throughput genomic studies have provided valuable insights into the molecular mechanisms involved in melanoma progression [8-10]. Malignant melanoma is recognized as one of the most aggressive forms of skin cancer, known for its high mortality rate attributed to its increased metastatic potential and increased drug resistance. Early detection of the tumour and prompt removal are crucial for optimal management and improved outcomes. Newly developed genetic tests are of paramount importance for a more accurate prognosis of cutaneous melanoma. Treatment of early-stage melanomas is surgical removal of the tumour; while for late stage melanomas, surgery may be required as well as additional treatments such as immunotherapy or targeted therapy drugs [11, 12]. However, there are no standard of care for systemic therapy that offer significant prolongation of survival for most patients with metastatic melanoma [13, 14]. Therefore, studying metastasis specific biomarkers is crucial for identifying new pathological parameters that can aid the design therapeutic agents that contribute at slowing down or inhibiting melanoma cell invasion and metastasis. In our global gene-expression studies, we observed a significant increased osteopontin (OPN) expression in a series of primary melanoma samples associated with poor clinical outcome [15]. OPN plays a critical role in cancer progression and formation of metastasis in various malignancies including malignant melanoma [16-19]. Previous reports have been indicated that elevated OPN is correlated with tumour invasion, metastasis and high-grade malignancies [15, 20-22].

The primary objective of our study was to assess the expression of osteopontin both mRNA and protein levels in primary melanoma tissues and melanoma cell lines. Additionally, we aimed to investigate the correlation between OPN expression and clinical-pathological parameters in melanoma patients to better understand the potential impact of molecular alterations on clinical outcomes. In this study, we also aimed to examine the impact of osteopontin expression on cell proliferation and invasion by inhibiting OPN expression using small interfering RNA (siRNA). Furthermore, our objective was to elucidate the role of osteopontin in melanoma progression.

Background

Molecular background of malignant melanoma

In addition to its aggressive nature, malignant melanoma is also known for its heterogeneous biological behavior, with multiple signaling pathways involved in its molecular pathogenesis. In recent decades, numerous important molecular pathways have been discovered to be implicated in the initiation, proliferation, survival, progression, and invasion of the disease, including mitogen-activated protein kinase (MAPK) pathway, phosphatidylinositol-4,5-bisphosphate 3-kinase (PI3K)/AKT pathway, cell-cycle regulation pathway, epigenetic factors, and some other signaling pathways [23, 24].

Based on the literature, approximately 10% of melanoma patients have family history of the disease [25]. It is well known that the most common genetic alterations involved in the development of hereditary melanoma affect genes that regulate the cell cycle, such as CDKN2A (cyclin-dependent kinase inhibitor 2A), CDK4 (cyclin-dependent kinase 4). Additionally, genetic variation in the MC1R (melanocortin 1 receptor) gene responsible for skin pigmentation have been indicated. Furthermore, the genetic disorder xeroderma pigmentosum (XP) that which impairs disrupts the proper repair of UV induced DNA damage, is also associated with a higher mutation rate in melanoma [26-29].

The two main signaling cascades in melanoma include: the MAPK pathway, which is mainly responsible for cell proliferation, and the PI3K/AKT pathway, which plays an important role in tumour cell survival. MAPK signaling cascade is activated in the most of melanomas through somatic mutations in the *NRAS*, *BRAF*, and *MEK1/2* genes. PI3K is a key regulator of melanocyte biology and is frequently activated by the mutation in PTEN expression which negatively regulates the pathway. Through molecular interactions between the members of the two signaling pathways tumorigenesis can be also enhanced, effecting cellular growth, chemoresistance, invasion, migration and cell cycle dysregulation (**Figure 3**) [30]. Mutations

in tumour suppressor genes that interfere with cell cycle regulation, such as *CDKN2A*, may promote the development of melanoma with an aggressive phenotype via the p16INK4A-cyclin D-CDK4/6-RB signaling pathway.

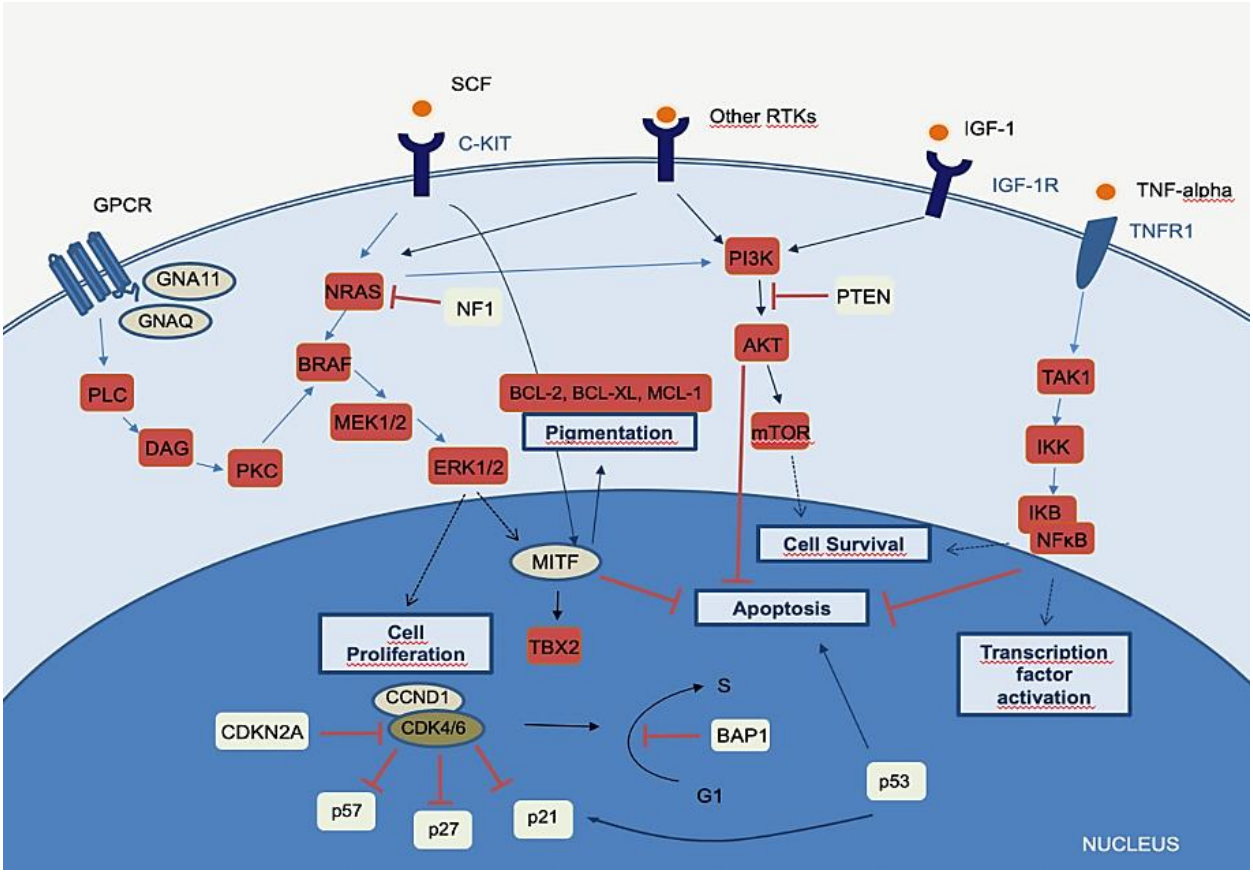

Figure 3. Major pathways involved in melanoma. [29]

Other important pathways in melanoma are the canonical WNT (wingless-type MMTV (mouse mammary tumour virus) integration site family) -β-catenin and MSH (melanocyte-stimulating hormones) -PKA (protein kinase A) -MITF (microphthalmia-associated transcription factor) signaling which also contribute to melanoma proliferation and pigmentation [24, 31, 32]. MITF is a transcription factor whose expression is frequently increased in melanoma cells. Its role in melanoma progression is complex and controversial, as it can act both as an oncogene and in a tumour suppressive role. The identification of key driver mutations and their impact on the signaling pathways has significantly enhanced our understanding of the molecular background

of human malignant melanoma, consequently creating new dimensions for the treatment of the disease.

The role of biomarkers in cancer biology

During the last decades**,** important improvements cancer biology, genomics, and molecular technologies have led to the discovery of several new cancer biomarkers including human malignant melanoma. Common types of tumour biomarkers are classified as diagnostic, prognostic, and predictive. Diagnostic biomarkers are employed to detect and confirm the presence of tumours, enabling the early detection of potential recurrence, and guide treatment decisions. Prognostic biomarkers predict the probable course and possible outcomes of the disease, whereas predictive biomarkers are used to assess the probable response to a specific treatment. The prognostic biomarker categories are summarized in **Figure 4** for cutaneous melanoma [33, 34].

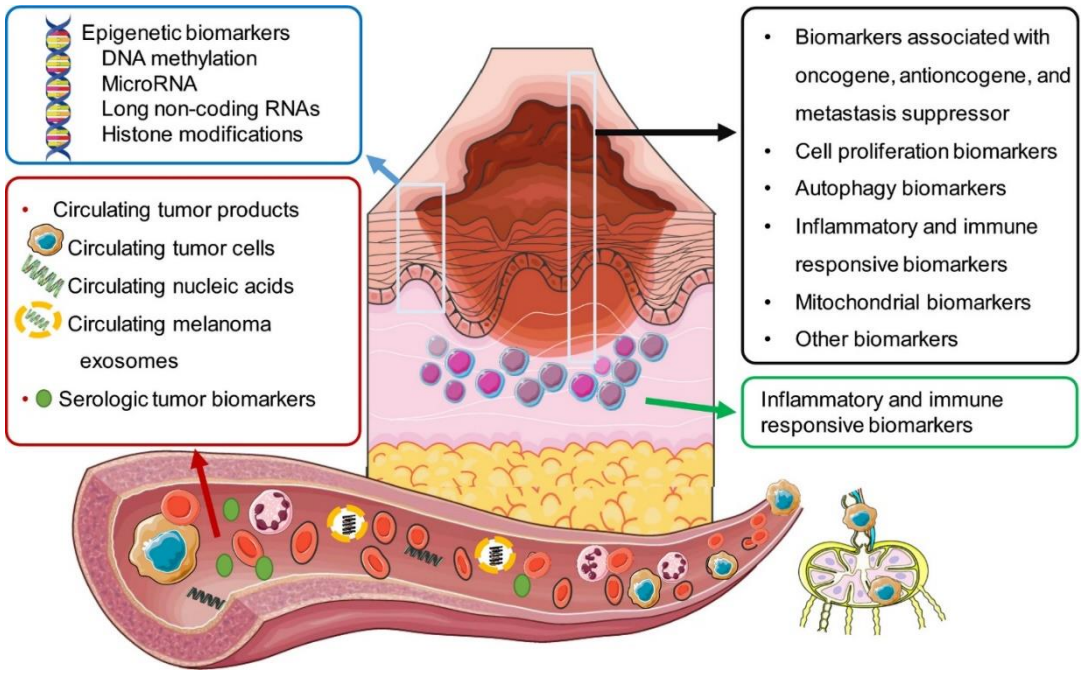

Figure 4. Schematic illustration of prognostic biomarkers for cutaneous melanoma [33].

Among the most extensively studied serological prognostic markers are S100 calcium-binding protein B (S100B), decreased vitamin D level, serum lactate dehydrogenase (LDH), hepatocyte growth factor (HGF), serum indoleamine 2,3-dioxygenase (IDO), eosinophil cationic protein (ECP) and melanoma inhibitory activity (MIA) [35-41].

The circulating tumour products (CTPs) can be divided into three subgroups: circulating tumour cells (CTCs), circulating nucleic acids, and circulating exosomes [42-46], all are important in the early diagnosis and to predict the prognosis of melanoma [47]. In addition, it can provide information about the presence of disseminated melanoma cells and may indicate a higher risk of metastasis [48].

Epigenetic events in melanoma play a dynamic role in the regulation of gene expression by modifying chromatin, including DNA methylation, covalent modifications to histones (such as acetylation or methylation), and regulation of mRNA translation through noncoding RNAs [49-52]. Key epigenetic events contributing to tumorigenesis in malignant melanoma include methylation, microRNA (miRNA), long noncoding RNAs (lncRNAs), and histone modification [53], these melanoma biomarkers are summarized by Thomas et al., Ghafouri-Fard et al., and Wilmott et al. [49-52].

Signaling pathway biomarkers in melanoma tissue are listed by Revythis, A., et al. highlighting the importance of mutations or overexpression of oncogenes inactivation of tumour suppressor genes [33, 54]. Recently, microarray-based gene expression profile (GEP) analysis has advanced in the understanding of melanoma-genesis, allowing to study the relationship between mRNA signatures and tumour progression. [55, 56]. Gerami and his team identified 28 prognostic- and 3 control genes and created skin and uveal melanoma signatures gene expression panel containing 31-gene (DecisionDx-Melanoma, Castle Biosciences Inc.). The majority of these genes had decreased expression in early melanomas, except for *SPP1* (osteopontin gene), *KRT6B* (Keratin 6B), and *EIF1B* (eukaryotic translation initiation factor 1B

gene), which are commonly overexpressed. The DecisionDx-Melanoma gene panel is a validated test that was developed strictly predict the metastasis risk of patients with melanoma. Previously published studies have shown that this gene panel has strong independent prognostic power [9, 57-59].

DNA biomarkers, especially mutated *BRAF* and *NRAS* genes, provide reliable associations with patient selection to targeted therapy and predict response to the treatment. ctDNA and miRNAs or lncRNAs contribute to the understanding of the disease's the pathophysiology, and enable the serial, non-invasive sampling for disease monitoring [54]. **Table 1** summarizes the key biomarkers for melanoma, based on Belter et al [60].

Table 1. Summary of the main biomarkers in malignant melanoma [60].

	Biomarkers*	**Correlation**
Enzymes	LDH	prognosis, tumour stage, survival rate
	Tyrosinase	poor prognosis, survival rate, overall survival
	Cox-2	*Breslow index*, tumour progression
	MMP-1, MMP-3	disease-free survival
	MMP-9	disease, poor prognosis
	MMP-2	tumour progression
	MMP-12	overall survival
	MMP-23	progression-free survival
	MT1-MMP	tumour progression
	TIMP-1	survival
	IDO	survival
	Cathepsin K	overall survival
	CD10	disease
Secreted proteins/antigens	VEGF	tumour stage and progression, survival
	Osteopontin	Breslow index, survival, poor prognosis
	IL-8	disease stage, survival
	Galectin-3	poor prognosis, tumour progression
	YKL-40	tumour stage and progression, poor prognosis
	MIA	survival poor prognosis
	C-reactive protein	survival tumour progression
	sICAM, sVCAM	survival
	CEACAM	tumour stage and progression, overall survival
	CYT-MAA	tumour progression
	MAGE	tumour progression
	MART-1	tumour stage
	TA90 antigen	survival, recurrence
S100 Proteins	S100B	tumour stage, survival, recurrence
Progenitor/stem cell-like markers	SOX protein family	disease
Metabolites	5-S-cysteinyl- DOPA	poor prognosis, response to treatment
	L-DOPA/L-tyrosine	tumour burden and progression
	6H5MI2C	Breslow index
Nucleic acids	miRNA-221	Breslow index
	miRNA-29c	overall survival

*Biomarker abbreviations are listed in the list of abbreviations.

Osteopontin and cancer progression

Osteopontin (OPN) also known as SPP1 (secreted phosphoprotein 1), or ETA-1 (Early T-lymphocyte Activation 1 protein) that was first identified in bone tissue. OPN is a multifunctional extracellular matrix protein comprising 314 amino acids and is encoded by the SPP1 gene, which is located on human chromosome 4 [61, 62]. OPN is produced by various cell types, including immune cells, osteoclasts, osteoblasts, epithelial cells and endothelial cells, and overexpressed in various types of cancer including breast, colorectal, gastric, liver, pancreas, lung, and melanoma [16, 18, 63]. It has been demonstrated that OPN plays an important role in cancer cell adhesion, cell motility, and survival. Extensive microarray analysis of melanoma has indicated that OPN has a serious role in melanoma progression. Published data suggests that OPN overexpression frequently associated with enhanced tumour invasion, metastasis and high-grade malignancies [63-65].

Signaling pathways that involve osteopontin are complex and contribute to the aggressive behavior of cancer cells. Regarding its biological functions, OPN enhances the survival of tumour cells through the interaction on CD44 variant (CD44v6/7 and v10) on the cell surface [66, 67]. Additionally it can also promote tumour metastasis through its interaction with integrins (αvβ1, αvβ3, αvβ5, α5β1) (**Figure 5**) [68, 69]. However, the molecular mechanism of OPN promoted progression of cutaneous melanoma is still not discovered. Recently, OPN has gained recognition as a significant cancer biomarker. Its role in the integrin-NF-κB/HIF-1α and PI3K/AKT pathways has become a focus of ongoing research, highlighting its importance in cancer-related processes [70-72]. The activation of the NF-κB and PI3K/Akt cascade induced by OPN may promote cell survival, inflammatory processes, proliferation and resistance to apoptosis. OPN signaling can activate the MAPK/ERK pathway, contributing to enhanced cell proliferation and survival [73]. OPN promotes cancer cell invasion by enhancing cell motility and extracellular matrix degradation. It also enhances the formation of premetastatic niches in

distant organs, facilitating metastasis. It triggers angiogenesis by stimulating the migration of endothelial cells and promoting the secretion of angiogenic factors. Elevated levels of OPN in cancer tissues or serum are associated with poor prognosis in various cancers, including melanoma [16]. Several studies suggest that OPN would be a specific target for cancer therapy [16, 17, 19]. Blocking OPN signaling pathways may inhibit tumour progression and enhance the effectiveness of cancer therapies. OPN has been associated in treatment resistance in leukemia, lung, breast, colorectal and head and neck cancer [63, 74, 75]. Our research group demonstrated that decreased OPN expression in resistant melanoma cell lines could potentially serve as an early marker of BRAF inhibitor (PLX4720) resistance [76].

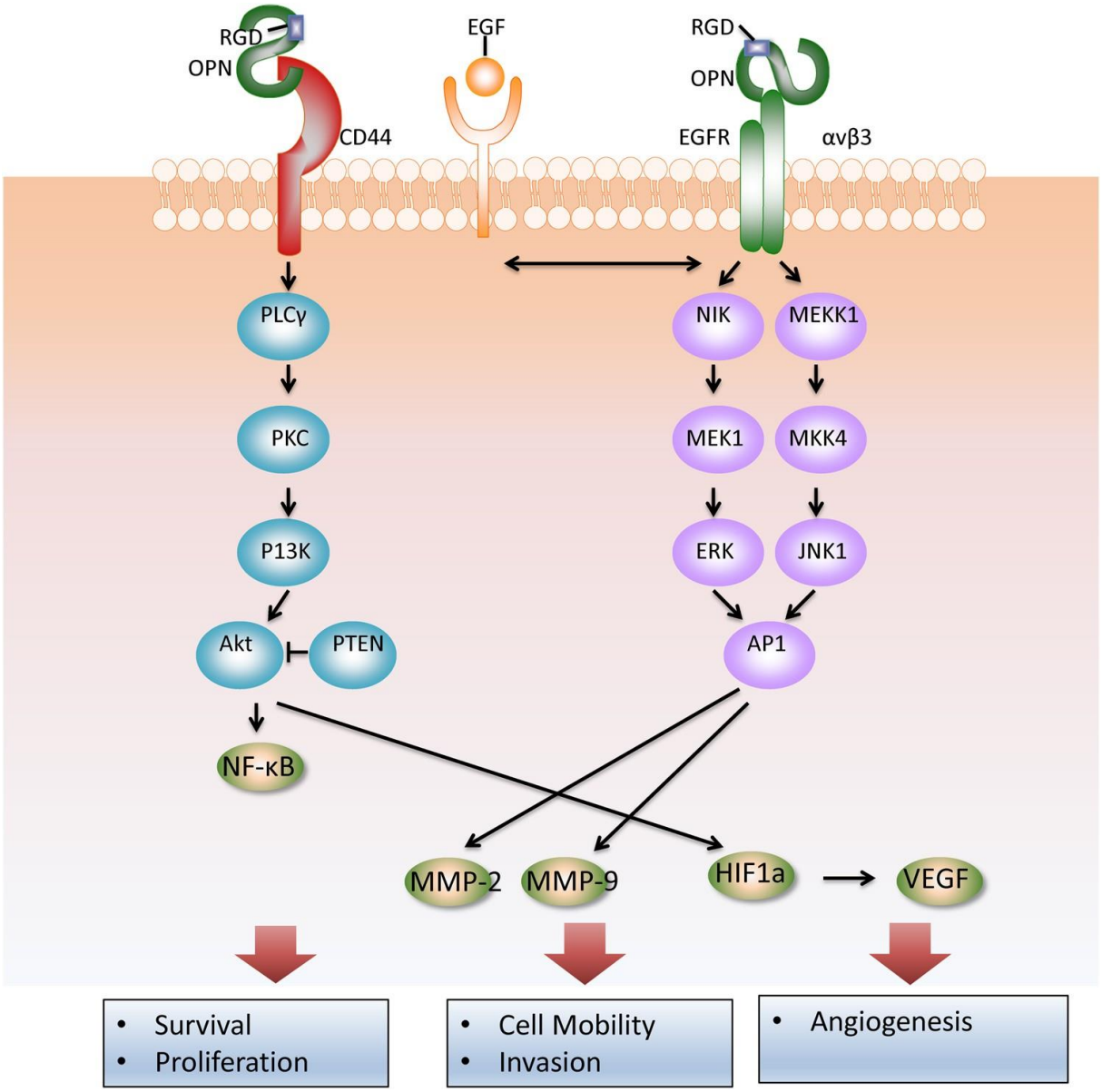

Figure 5. Osteopontin signaling in tumour progression of cancer cells [16]

It is now widely accepted that inhibition of OPN expression through RNA interference (RNAi) holds promise strategy for cancer treatment [17, 77-79]. Cho et al. presented that silencing of OPN expression using siRNA targeting OPN resulted in suppression of tumour growth in two non-small cell lung cancer (NSCLC) xenograft models which is promising for lung cancer therapy [79]. Tang and coworkers demonstrated that silencing of OPN expression in the liver is one of the important strategies for the management of liver fibrosis [80]. Nemoto and

researchers demonstrated that osteopontin deficient B16 melanoma cells have showed reduced metastasis to soft tissues and bone [81]. Taken together, studies have demonstrated that OPN have exhibits antimetastatic and antitumorigenic effects in various cancers [79, 82]. However, no data are currently available for malignant melanoma, indicating the need of future research to determine the significance of OPN in siRNA-based treatments for melanoma.

Current and novel targeted therapies in melanoma

Surgically removing early-diagnosed melanoma is a highly effective method for preventing disease recurrence. In the case of advanced-stage melanoma, the therapeutic standard of care used to be chemotherapy with dacarbazine (DTIC) and high-dose interleukin-2 (IL-2) were the therapeutic standard of care until the approval of the RAF inhibitor vemurafenib and the CTLA-4 antibody ipilimumab in 2011. The discovery of melanoma driver genes has played a crucial role in the development of targeted therapies. Since then, multiple target specific therapies and immune checkpoint inhibitors have been approved for clinical use in the treatment of metastatic melanoma (**Figure 6**). One of these monoclonal antibodies, nivolumab, which alone or in combination with ipilimumab, has markedly increased progression-free survival in patients with metastatic melanoma [83]. In 2014, the combination of the BRAF inhibitor dabrafenib and the MEK (MAPK kinase) inhibitor trametinib was approved by the Food and Drug Administration (FDA) for the treatment of BRAF-mutant metastatic melanoma. Studies have shown that combining them improved response rates and delayed the development of resistance [84]. Subsequently, combination therapies approved for the adjuvant treatment of melanoma have been shown to promote recurrence-free survival in high-risk patients [85]. Today, the effectiveness of cancer treatment requires two or more combined drugs involving several mechanisms. Successful therapeutic interventions present oncologists with new challenges due to the emergence of drug resistance and the genetic changes that underlie it. On the one hand,

to avoid this, combination therapies have been developed that target several points of the same signaling pathway simultaneously. On the other hand, the molecular profiling of the primary tumour should be replaced by continuous monitoring.

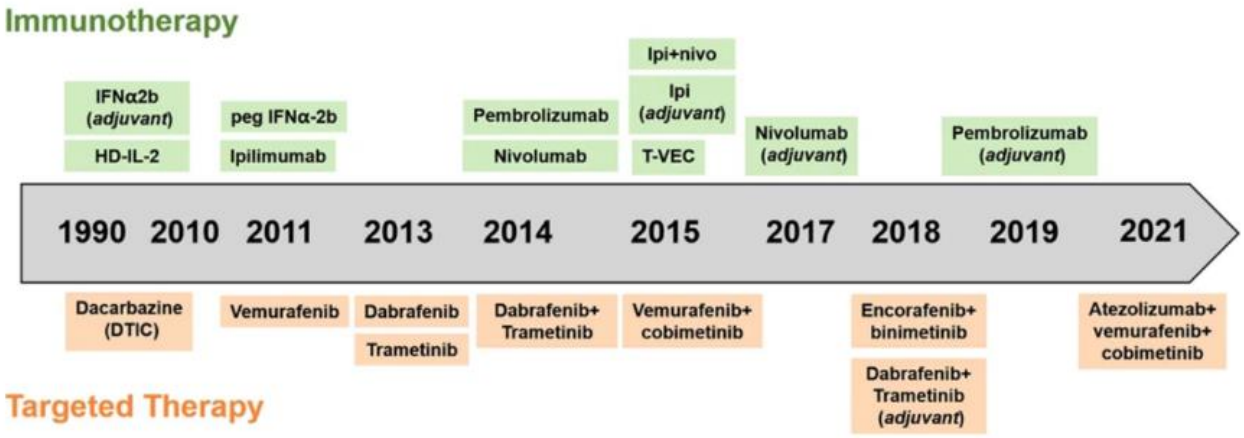

Figure 6. Timeline of FDA-approved drugs for advanced melanoma [24].

Besides, the most important advances in molecular biology has been the discovery that small interfering RNAs (siRNAs) are able to regulate gene expression by RNA interference (RNAi). RNAi is a biological process in which RNA molecules inhibit gene expression or translation, through a process of damage to specific mRNA molecules. There are two types of small ribonucleic acid (RNA) molecules that play a key role in RNA interference, namely microRNA (miRNA) and small interfering RNA (siRNA). RNAi mechanism is activated by the enzyme Dicer which cuts double-stranded RNAs (dsRNAs) into short double-stranded siRNAs of 21–25 nt. The miRNA or siRNA then binds to the RNA-induced silencing complex (RISC), an enzyme-containing molecule. The miRNA-RISC or siRNA-RISC complex binds to target, or complementary, messenger RNA (mRNA) sequences, resulting in the enzymatic cleavage of the target mRNA which is deactivated or silenced (**Figure 7**) [86]. Because the targeted mRNA is either degraded or cannot undergo translation, leading to reduced expression of the gene.

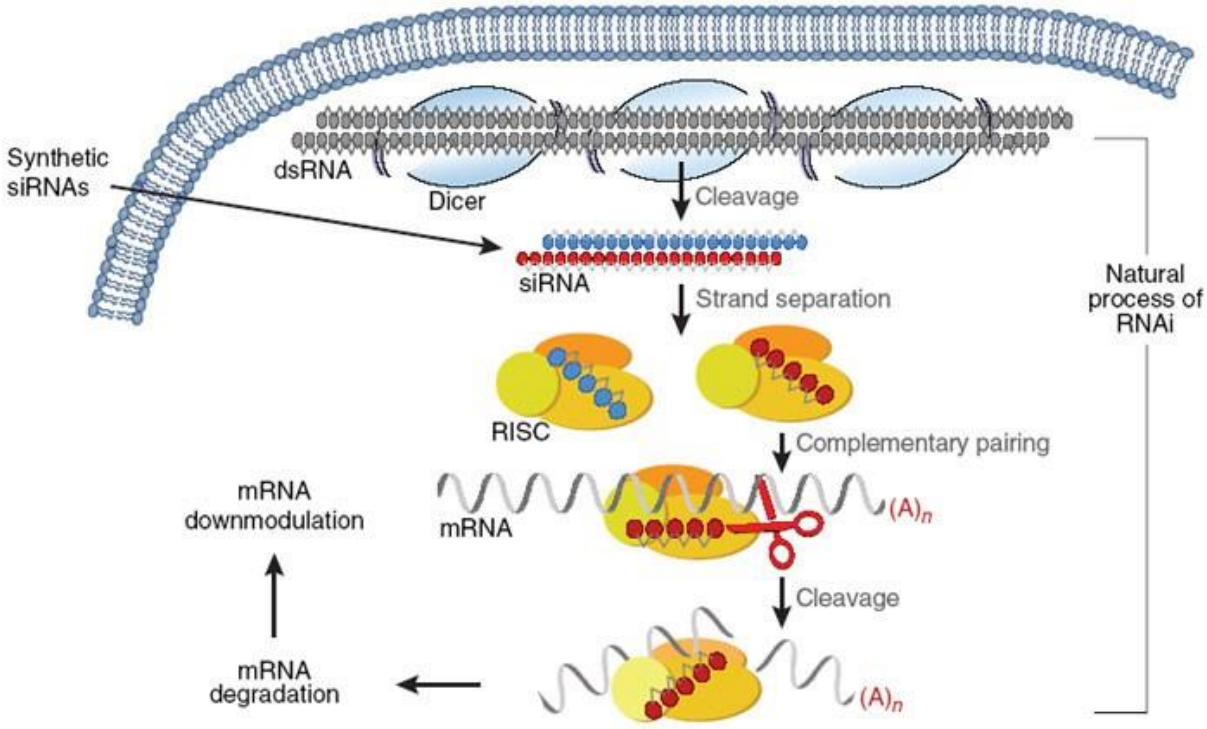

Figure 7. Mechanism of RNAi-mediated silencing [87].

RNAi has shown promising therapeutic results for a variety of diseases, including cancers, viral infections, ocular conditions, genetic disorders and cardiovascular diseases and is therefore a highly effective research tool [87-89]. In 2018, the FDA approved the first RNAi drug for sale due to its effectiveness and safety [90]. siRNA-based treatments can be hopeful gene-related therapeutics for cancer because many genes are upregulated at some stages in tumour initiation and contributed to cell proliferation and tumour progression. Targets of siRNA-based therapeutics are separated into three major groups in cancer treatment as presented in **Figure 8**, including molecules that are participated in carcinogenesis, gene products that engaged in tumour-host interactions, and gene products that are involved in tumour resistance to chemotherapeutics [91, 92]. siRNA targets may include oncogenes KRAS and MYC, whose inhibition of expression may suppress cancer cell proliferation and induce cell death, respectively [93, 94]. The inhibition of VEGF, which plays a role in promoting angiogenesis, can block blood supply, leading to tumour starvation [95]. siRNA targeting anti-apoptotic proteins such as Bcl-2 may promote cancer cell death [96]. In gastric tumours, inhibition of ANO9, which plays a role in evading the tumour immune system, induced tumour cell apoptosis and caused reduced migration and invasion, suggesting it could be a potential biomarker for

gastric tumours [97]. While siRNA-based cancer therapies show promise for the treatment of tumours, they are still an active area of research and ongoing clinical trials are needed to establish their safety and efficacy for widespread clinical application.

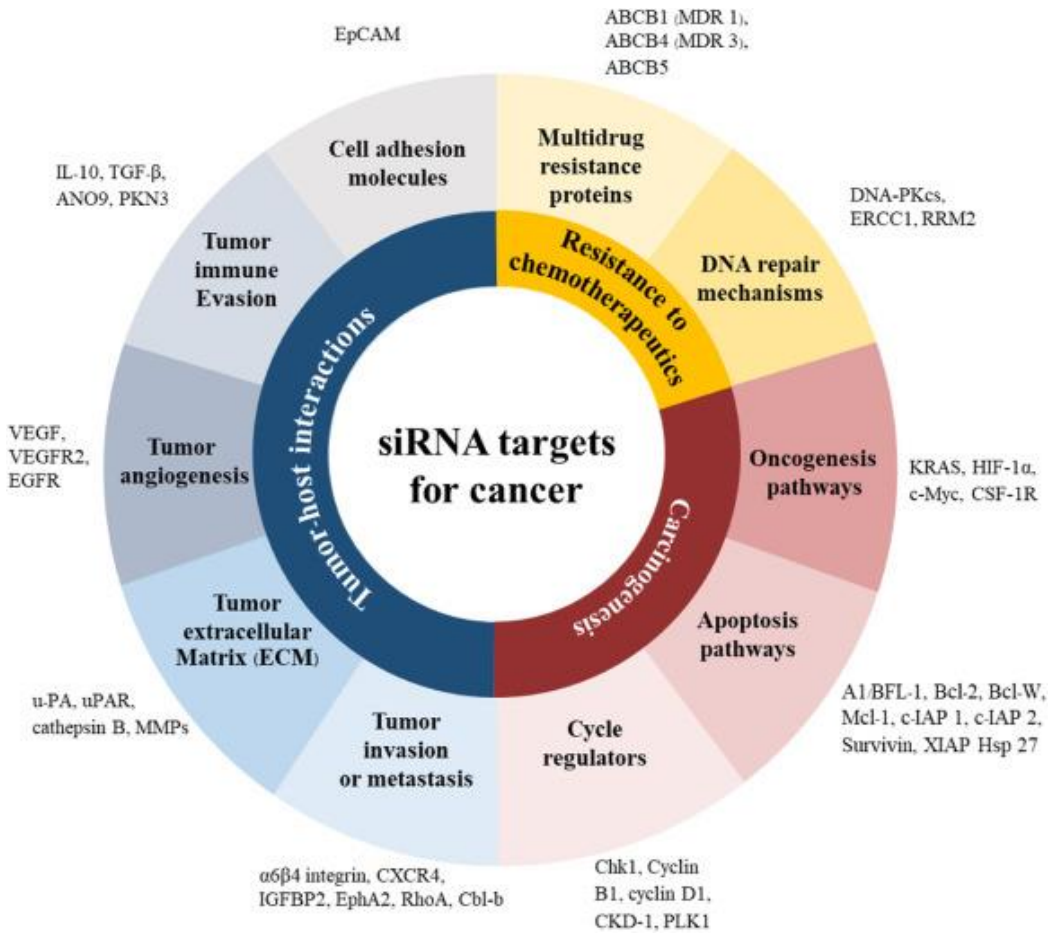

Figure 8. Major siRNA targets for cancer treatment [91].

Objectives

The role of osteopontin (OPN) in tumorigenesis is complex, and likely exhibits diverse effects in different types of malignancies. The objective of this study was to deeper understand the role of OPN expression during melanoma progression. Our first aim was to investigate OPN expression in a series of primary tumour tissues with distinct biological behavior. Subsequently, our second goal was to examine the impact of inhibiting OPN expression using small interfering RNA (siRNA) on cell proliferation and invasion, aiming to elucidate the molecular mechanisms underlying OPN's involvement in cutaneous melanoma progression.

In details, our study aimed to accomplish the following objectives:

1. Determine OPN expression at both mRNA and protein levels of various subtypes of primary melanoma tissues using immunohistochemistry on tissue microarrays, and quantitative real-time polymerase chain reaction (qRT-PCR). Additionally, we aimed to correlate the expression patterns with the clinical-pathological parameters of the melanoma patients.

2. Assess the mRNA and protein levels of OPN expression in melanoma cell lines derived from primary and metastatic tissues.

3. Inhibit OPN expression using siRNA in specific melanoma cell lines that exhibit high OPN expression. Subsequently, assess the impact of transfection on cell proliferation and invasion.

4. Investigate the protein expression patterns of the parental and siRNA silenced melanoma cell line pairs that were developed form the same patients primary and metastatic tumours. The investigation will be carried out using proteome profile analysis.

Materials and methods

Melanoma tissue samples

Melanoma tissues were obtained from the Department of Dermatology, University of Debrecen, Hungary. This study received approval from the Regional and Institutional Ethics Committee of the University of Debrecen (Hungary) and the Medical Research Council (Hungary). The research was conducted in compliance with all relevant regulations and guidelines (DE RKEB/IKEB: 2836/2008; RKEB/IKEB: 4820-2017; TUKEB (MRC): 25364-1/2012/EKU (449/PI/12). Written informed consent was obtained from all participating patients. Lesions were diagnosed based on formalin-fixed paraffin-embedded (FFPE) tissue sections stained with haematoxylin-eosin (H&E) and the classification was performed according to the latest edition of TNM staging system [98]. It is important to note that the examination of OPN expression in melanoma tissues was not conducted simultaneously; therefore, the studied set of melanoma samples did not completely overlap.

The clinical-pathological parameters of the tumours are presented in **Table 2** and **Table 3**. **Table 2** summarizes melanoma tissue samples that were analyzed during our first study (Kiss T et al. Tumor Biology volume 36, pages 7841–7847; 2015). A total of 93 primary melanoma tissues were analyzed using immunohistochemistry, 28 primary tumours were evaluated by qRT–PCR, and 14 primary tissues were investigated using both methods [99]. Immunohistochemistry was performed on tissue microarray following the described protocol.

Table 3 summarizes primary melanoma and melanoma metastases tissue samples that were analyzed by qRT-PCR during our study published in 2021. in Pathol Oncol Res. (2021; 27: 581395. entitled “Silencing Osteopontin Expression Inhibits Proliferation, Invasion and Induce Altered Protein Expression in Melanoma Cells”).

Table 2. Clinical-pathological parameters of primary melanomas analyzed during the study published in Tumor Biology in 2015 [99].

Variables	Number of tumours analyzed by	
	IHC[1]	qRT- PCR
All patients	93	28
Histological subtype		
SSM[2]	50	18
NM[3]	43	10
Gender		
Female	56	14
Male	37	14
Age (years)		
20-50	23	6
≥50	70	22
Breslow thickness (mm)[4]		
≤2.00	36	12
2.01-4.00	29	4
>4.01	28	12
Clark's level		
I-III (early)	48	13
IV-V (late)	45	15
Ulceration		
Absent	57	14
Present	36	14
Localisation		
Extremity	38	16
Trunk	42	10
Head	13	2
Metastasis formation[5]		
Absent	56	13
Present	37	15
Patient's survival		
Alive	54	18
Exitus	39	10

[1]immunohistochemistry, [2]superficial spreading melanoma, [3]nodular melanoma; [4]thickness categories are based on the current staging system; [5]patients with at least 5-year follow-up period were included

Table 3/A. Clinical–pathological data of primary melanoma tissue samples analyzed during the study published in the Pathology and Oncology Research in 2021 [100].

Sample	Sex	Age at diagnosis (year)	Histological subtype	Breslow thickness (mm)	Clark stage	TNM status
P04	F	40	SSM	7	IV	T4bN0M0
P05	M	52	SSM	3.2	IV	T3bN0M0
P06	M	74	SSM	5	III–IV	T4bN0M0
P08	M	41	SSM	14	V	T4b2bM3
P09	F	54	SSM	11	n.d.	T4N2
P10	M	71	SSM	0.15	III	T1aNxMx
P12	M	68	SSM	3.5	III–IV	T3bN0M0
P13	M	51	SSM	2.42	III	T3aNxMx
P14	F	62	SSM	0.57	III	T1aN0M0
P15	M	53	SSM	0.72	III	T1aN0M0
P18	M	51	SSM	1.33	III	T2aN0M0
P19	F	54	SSM	0.65	III	T1aN0M0
P23	F	70	SSM	0.36	III	T1aN0M0
P24	F	70	SSM	0.24	III	T1aN0M0
P25	F	44	SSM	0.24	III	T1aN0M0
P26	M	47	SSM	3.14	III	T3aN0M0
P31	F	75	SSM	3	IV	T3bN0
P32	M	73	SSM	2.8	IV	T2aNx
P34	M	51	SSM	3.2	IV	T3aN0
P35	F	86	SSM	2.4	IV	T3bN0
P36	F	72	SSM	2.4	IV	T3aN0
P01	F	71	NM	7	IV	T4bN0M0
P02	M	38	NM	12	IV	T4bN0M0
P03	F	77	NM	12	V	T4bN3M0
P07	M	44	NM	25	V	T4bN0M0
P11	M	63	NM	8	V	T4bN0M0
P17	F	61	NM	2.64	III	T3aN0M0
P22	F	44	NM	3.72	III	T3aN0M0
P27	M	72	NM	3.6	III	T3bNxMx
P28	F	83	NM	3.5	IV	T3b
P33	M	77	NM	2.2	IV	T3bN0

F: female; M: male; n.d.: no data available; SSM: superficial spreading melanoma; NM: nodular melanoma.

Table 3/B. Clinical–pathological data of melanoma metastasis tissue samples analyzed during the study published in the Pathology and Oncology Research in 2021 [100].

Sample	Sex	Age at diagnosis (year)	Localization
M01	M	n.d.	distant
M02	n.d.	n.d.	distant
M03	M	81	rSC/C
M04	M	75	rLN
M05	F	74	rSC/C
M06	F	30	rLN
M07	M	72	rLN
M08	n.d.	n.d.	distant
M09	M	65	rLN
M10	M	52	rSC/C

rLN: regional lymph node; rSC/C: regional (sub)cutaneous; n.d.: no data available.

Melanoma cell lines

The experiments were conducted using primary melanoma cell lines derived from the following sources: WM35, WM793B, WM3211, WM902B, M35/01, WM1361, WM1366, HT199, WM39, WM3248, WM278, WM983A. Metastatic melanoma cell lines used were: WM1617, WM983B, SK-MEL-28, A2058, HT168-M1, M24, M24met, Melur. These cell lines were obtained from the American Type Culture Collection (Manassas, Virginia, USA) and the Coriell Institute for Medical Research (Camden, New Jersey, USA). The HT199 and HT168-M1 melanoma cell lines were developed at the 1st Institute of Pathology and Experimental Cancer Research, Semmelweis University, Budapest, Hungary [101]. The cell lines were cultured in RPMI 1640 medium (Lonza Group Ltd, Basel, Switzerland) or MCDB153-L15 medium (Sigma-Aldrich Co. LCC, St Louis, Missouri, USA) and supplemented with 10%

foetal bovine serum (Gibco, Carlsbad, California, USA) at 37°C in an atmosphere containing 5% CO_2. Characteristics of the cell lines are summarized in **Table 4**.

Table 4. Characteristics of human melanoma cell lines.

Cell line	Origin[1]	Growth Phase[2]	Histologic Type3	BRAF mutation status	NRAS mutation status
WM35	primary	RGP/VGP	SSM	V600E	wt
WM793B	primary	RGP/VGP	SSM	V600E	wt
WM3211	primary	RGP/VGP	SSM	wt[4]	wt
WM902B	primary	VGP	SSM	V600E	wt
M35/01	primary	VGP	SSM	V600E	wt
WM1361	primary	VGP	SSM	wt	Q61L
WM1366	primary	VGP	SSM	wt	Q61L
HT199	primary	RGP	NM	V600E	wt
WM39	primary	VGP	NM	V600E	wt
WM3248	primary	VGP	unknown	V600E	wt
WM278[5p]	primary	VGP	NM	V600E	wt
WM1617[5m]	metastasis	-	-	V600E	wt
WM983A[6p]	primary	VGP	unknown	V600E	wt
WM983B[6m]	metastasis	-	-	V600E	wt
SK-MEL-28	metastasis	-	-	V600E	wt
A2058	metastasis	-	-	V600E	wt
HT168-M1	metastasis	-	-	V600E	wt
M24	metastasis	-	-	wt	Q61R
M24 met	metastasis	-	-	wt	Q61R
Melur	metastasis	-	-	wt	wt

[1]origin of cell lines; [2]RGP: radial growth phase, VGP: vertical growth phase; [3]SSM: superficial spreading melanoma, NM: nodular melanoma; [4] wt: wild-type, n.d.: no data; [p]primary tumour-derived cell line with metastatic pair from the same patient; [m]metastatic pair of primary tumour derived cell line

Detection of BRAF and NRAS mutation

The majority of melanoma cell lines had their *BRAF* and *NRAS* mutation status had previously tested and provided by ATCC or Coriell Institute for Medical Research. For six specific cell

lines (A2058, HT168-M1, M24, M24met, HT199 and WM902B) the mutations in *BRAF* codon 600 and *NRAS* codon 61 were determined by melting curve analysis using fluorescent probes on the LightCycler real time PCR System (Roche Diagnostics GmbH, Mannheim, Germany). Primers and probes were obtained from TIB Molbiol GmbH (Berlin, Germany). The reaction procedure was carried out according to the previously described method [102].

RNA extraction and qRT-PCR analysis

The RNeasy Plus Mini Kit (Qiagen GmbH, Hilden, Germany) was used to isolate total RNA from melanoma cell lines following the manufacturer's protocol. The concentrations of the RNA samples were measured using a NanoDrop ND-1000 UV-Vis spectrophotometer (NanoDrop Technologies, Wilmington, DE, USA). Reverse transcription (RT) was carried out on 600 ng total RNA using the High-Capacity cDNA Reverse Transcription Kit, following the manufacturer's instructions (Life Technologies Corporation, Carlsbad, California, USA).

TaqMan one-step RT-PCR was employed to quantify the mRNA level of the *OPN* gene in 28 primary melanoma tissues. Each reaction consisted of 150 ng of total RNA from the samples, and reactions were performed in triplicate on ABI-PRISM 7000 instrument (Applied Biosystems, Carlsbad, CA, USA). PCR Master Mix and assay (Hs00167093_m1 OPN targeting the exon 3-4 boundary) were obtained from Life Technologies.

In our subsequent studies, the relative expression level of the *OPN* gene was assessed through quantitative real-time PCR (qRT-PCR) using the LightCycler® 480 Real-Time PCR System (Roche Diagnostics, GmbH, Mannheim, Germany). This analysis was conducted on 34 primary and 12 metastatic melanoma tissues, 12 primary melanoma- and 8 melanoma metastasis originated melanoma cell lines (refer to **Table 3** and **Table 4**). The qPCR reactions were performed using SYBR premix Ex Taq (Takara Holding Inc., Kyoto, Japan) master mix.

The raw PCR data were analyzed using the Livak method ($2^{-\Delta\Delta Ct}$), GAPDH (glyceraldehyde-3-phosphate dehydrogenase) was used as an internal control gene. Pooled nevi (n=8) and cultured melanocyte were utilized as the calibrator samples [103].

Immunohistochemistry on melanoma Tissue Microarray

Immunohistochemistry was performed on 93 FFPE melanoma tissue sections [104]. The clinical-pathological data of the primary melanomas are summarized in **Table 2**. Four μm tissue sections of the original melanoma blocks were initially stained with haematoxylin-eosin and then examined by pathologists. The pathologists selected the specific area to be automatically punched using the fully automated tissue microarray (TMA Master, Carl Zeiss, Jena, Germany). Tumour cores measured 1 mm (triplicate) were obtained from each melanoma tissue block. Serial sections of 4 μm were sliced from the TMA blocks and used for immunohistochemical investigations. Microarray sections were stained with haematoxylin-eosin and validated the sample spots for tumour cell content under a microscope. After deparaffinization, endogenous peroxidases were blocked by treating the samples with 1% H_2O_2 for 10 min at RT. Non-specific binding sites were subsequently blocked. Antigen retrieval was performed by heating the samples in 1 mM boiling citrate buffer (pH 6.0) for 3 minutes. The primary antibody, rabbit polyclonal anti-osteopontin IgG (Thermo Scientific, Waltham, Massachusetts, USA) was added at a 1:20 dilution and incubated for 1 hour at room temperature. Following the primary antibody incubation with, the samples were stained using the peroxidase/DAB based Envision detection system (DAKO Inc., Carpinteria, CA, USA) and VIP peroxidase substrate kit (Vector Laboratories LTD, Peterborough, UK). Nuclei were counterstained with methyl green (Vector Laboratories LTD). Negative controls were prepared by omitting the primary antibody. The HeLa cervical cancer cell line served as the positive control in this study. The tissue microarray slides were digitized using MiraxScan slide scanning device (Carl Zeiss), following the previously described method [105]. Digital images were viewed using MiraxViewer software

(Carl Zeiss) and evaluated by two dermatopathologists who were blinded to the tissues clinical-pathological characteristics. We implemented two scores for tissue characterization: 1.) tumour cell proportion score and 2.) intensity staining score. The proportion score determined the fraction of positively stained tumour cells based on the following criteria: 0 = none, 1+ = <5%, 2+ = 5-50%, 3+ = >50%. The estimated average staining intensity of the positive tumour cells was expressed as follows: 0 = none, 1+ = weak, 2+ = moderate, 3+ = strong (**Figure 9**).

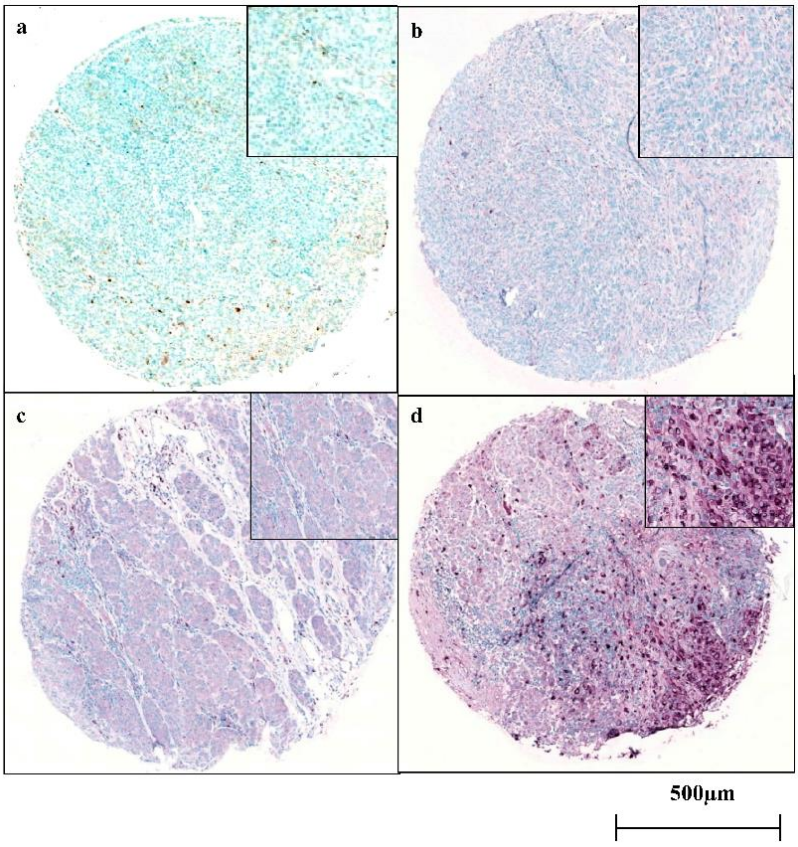

Figure 9. Immunostaining intensity scores for primary melanoma tissues. *(a) no staining of OPN protein in melanoma samples (0); (b) weak staining (1+); (c) medium staining (2+), and (d) strong staining (3+).*

Indirect immunofluorescence

Melanoma cells were cultured on 8-well Lab-Tek chamber slides (Nalge Nunc International, Naperville, IL) in RPMI 1640 medium (Lonza Group Ltd, Basel, Switzerland) containing 10% FBS (Gibco, CA, USA) overnight. The cells were washed twice with PBS, followed by fixation

with acetone for 10 minutes and air drying. Subsequently, the cells were rinsed with PBS (15 minutes) and blocked with 5% BSA in PBS at room temperature for 30 minutes. Primary antibodies, including anti-OPN antibody diluted to 1:500 (Rockland Immunochemicals Inc., Limerick, PA) and anti-NF-κB p65 antibody diluted to 1:50 (Cell Signaling Technology Inc., Danvers, MA), were then incubated with the cells overnight at 4°C in a humidified container. After rinsing with PBS, the cells were incubated with DyLight488-conjugated anti-rabbit or DyLight594-conjugated anti-rabbit IgG (Vector Laboratories Ltd, Peterborough, UK) for 1 hour at room temperature. Following another round of PBS washing, the cell nuclei were stained with 4'6-diamidino-2-phenylindole (DAPI, Vector Laboratories Ltd, Peterborough, UK). Images were analyzed using a confocal laser scanning microscope (Zeiss LSM700, Carl Zeiss).

Cell proliferation assay during the siRNA experiment

To assess cell proliferation as an indicator of undesirable RNAi activity, the WST-1 Cell Proliferation Reagent (Roche Magyarország Kft., Budaörs, Hungary) was utilized according to the manufacturer's instructions. The measurements were performed 78 hours after siRNA transfection. Absorbance was recorded at 450 nm using a NanoDrop ND-1000 UV-Vis Spectrophotometer (NanoDrop Technologies), with the reference absorbance was set at 700 nm. Cell proliferation was determined by comparing the results to control cells. Each experiments were conducted independently and repeated at least three times.

In vitro invasion assay

Melanoma cell lines invasive capacity was determined using BD Biocoat Matrigel invasion chambers (pore size: 8 μm, 24-well; BD Biosciences, Bedford, Massachusetts, USA) as described before [106]. The upper chamber of the insert was filled with 500 μl of cell suspension in serum-free media (5×10^4 cells/well), while the lower chamber contained medium with 10%

FBS as a chemoattractant. The cells were incubated for 24 hours at 37°C. Non-invading cells were removed with a cotton swab, cells with invasive potential attaching to the lower layer of the membrane were fixed with methanol and stained with haematoxylin–eosin. The average number of invaded cells was determined in 7 different visual fields (at 200X magnification using a light microscope). The data are presented as the mean ± SD of three independent experiments.

siRNA experiments

The siRNA targeting human secreted phosphoprotein 1 (SPP1; OPN-targeting siRNA: ID: SI02757615) and the AllStars Negative Control siRNA (NC-siRNA ID: 1027281) were purchased from Qiagen GmbH (Hilden, Germany). The sequences of the OPN (or SSP1) specific siRNA are as follows:

sense:	5'GGCUGAUUCUGGAAGUUCUTT3'
antisense:	5'AGAACUUCCAGAAUCAGCCTG 3'

The sequence-specific siRNA was validated for its effectiveness the OPN gene expression by the manufacturer [107]. The siRNA showed no potential off-target mRNA effects, and exhibited a high degree of homology *(https://geneglobe.qiagen.com/product-groups/flexitube-sirna*). The specificity of the sequence was also verified using in the BlastN database. Consistent with published data, we used the lowest effective concentration (5 nM) of the siRNA in our experiments. Adjusting a concentration of 5 nM is a common approach to minimize potential off-target effects and non-specific binding [108].

One day prior to transfection, cells were seeded in 24-well plates at a density of $5x10^4$ cells per well and cultured in 500 µl of growth medium in each well. Importantly, the growth medium

did not contain antibiotics because it can interfere with the transfection process or affect viability. Cells were allowed to grow until cells reached a confluence level of 30-50%. This growth state is often preferred for transfection experiments to ensure that the cells are actively dividing and capable to effectively taking up the transfected genetic material. The transfection complexes were prepared using, siRNA (at a concentration of 5 nM) and lipofectamine 2000 transfection reagent (Invitrogen, Life Technologies, Carlsbad, CA, USA) resulting in a final volume of 100 µl, according to the manufacturer's protocol. The complexes were added to each well of the cell culture plate. After the 3 hours' incubation period, the medium was replaced with fresh medium in each well. By replacing the medium, any remaining transfection reagents that have not been taken up by the cells were removed, minimizing potential cytotoxic effects because it can be toxic to cells which continues to affect gene expression. Finally, this medium exchange support cell viability and helps maintain optimal conditions for further incubation. The cells were harvested 48 hours after transfection for subsequent analysis, and gene silencing efficacy was evaluated by qRT-PCR. All transfections were independently repeated three times.

Proteome array analysis

Melanoma cell lines were cultured in T25 flasks until reaching approximately 80% confluence, after cells were gently washed two times with 10 ml cold PBS. Next, 1 ml of RIPA Lysis and Extraction Buffer (Thermo Fisher Scientific Inc. Waltham, Massachusetts, USA) was added to each flask containing 20 µl of Halt™ Protease and Phosphatase Inhibitor Cocktail (Thermo Fisher Scientific Inc. Waltham). The cells were scraped using a cell scraper and the resulting cell lysates were transferred to a new Eppendorf tubes. The tubes were then incubated on a rocking shaker for 30 minutes at 4°C, and subsequently centrifuged at 13,000 rpm for 30 minutes at 4°C. The supernatants, excluding the pellet, were collected in new Eppendorf tubes. The protein concentration in the supernatants was measured using a Quick Start™ Bradford

Protein Assay (Bio-Rad Hungary Ltd. Budapest, Hungary) following the manufacturer's protocol.

Protein expression was assessed using a Proteome Profiler Human XL Oncology Array Kit (R&D Systems, Abingdon, United Kingdom) according to the manufacturer's instructions. This membrane-based antibody array allows for the detection of 84 cancer-related proteins between samples. Two-hundred µg cell lysates were incubated with each array overnight at 4°C on a shaker with rocking platform. On the following day, the cell lysates were removed, and the membranes were washed three times with wash buffer. Subsequently, the arrays were incubated with a detection antibody cocktail for 1 hour at room temperature on a rocking platform shaker, followed by three washes with wash buffer. A mixture of streptavidin – HRP mix (2 ml) was added to each membrane, and incubated for a 30 minutes, after which the membranes were washed three times. The protein spots labelled with streptavidin – HRP were visualized using Chemi Reagent Mix. The array spots were analyzed using ImageJ Lab 1.51 Software and normalized to the signal intensities of the positive control (1.51a, NIH, Bethesda, Maryland, USA) and evaluated by subtracting the background. Background subtraction was performed, and the intensity of the reference spots was considered as 100%.

The protein – protein functional associations were analyzed using STRING (Search Tool for the Retrieval of Interacting Genes) software, specifically utilizing database version 11.0 (http://string-db.org). STRING is a comprehensive database that contains information on both known and predicted protein-protein interactions. These interactions encompass both direct (physical) and indirect (functional) associations. The database integrates computational prediction, knowledge transfer between organisms, and interactions gathered from other primary databases *(https://string-db.org/cgi/about)*. STRING is being a web-based tool compiles associations between proteins from various sources [109].

Statistical analysis

Statistical analysis was performed using SPSS 22.0 (Statistical Package for the Social Sciences 22.0) software (SPSS Inc., Chicago, IL, USA). Fisher's exact and Mann-Whitney-Wilcoxon tests were employed to compare the OPN expression levels and the clinical-pathological data of primary melanomas. The relationship between the qRT-PCR data and clinical-pathological parameters of melanoma patients was analyzed using the Mann-Whitney-Wilcoxon tests. Fisher's exact was used for the statistical analysis of protein expression data.

Survival analysis was conducted using Cox regression analysis to evaluate predictors of survival. Survival times were calculated from the time of diagnoses to last follow-up or death of the patients. Logistic regression was employed to analyze association between prognostic factors and formation of metastasis. The Kruskal-Wallis test was used to determine significant differences among OPN gene expression in melanoma subgroups (SSM, NM and melanoma metastasis). A two-sided Mann-Whitney-Wilcoxon exact test was used to identify significant differences between primary and metastatic melanoma cell lines. Student's t-test was performed for the statistical analysis of the experimental siRNA data. All experiments were repeated at least three times, and the results are presented as the means ± standard deviation (± SD). A p value ≤ 0.05 was considered statistically significant.

Results

OPN mRNA expression in primary melanoma tissues

In the initial phase of the study, gene expression of *OPN* was performed using qRT-PCR in 28 primary melanoma samples. A significant increase (greater than twofold expression compared to the control) of the *OPN* gene expression was observed in 93% (26/28) of these melanoma samples. When examining the relationship between gene expression levels and clinical-pathological parameters, a statistically significant association was found between relative gene expression of the *OPN* gene and Breslow's thickness (greater than 4.00 mm), presence of ulceration on the tumour surface and tumour stage (Clark levels IV and V). **Figure 10** illustrates the notable differences between the clinical-pathological parameters and gene expression levels. The mRNA expression of *OPN* was significantly higher in thicker melanomas and in lesions with ulceration, indicating that OPN expression is predominantly present in advanced-stage tumours.

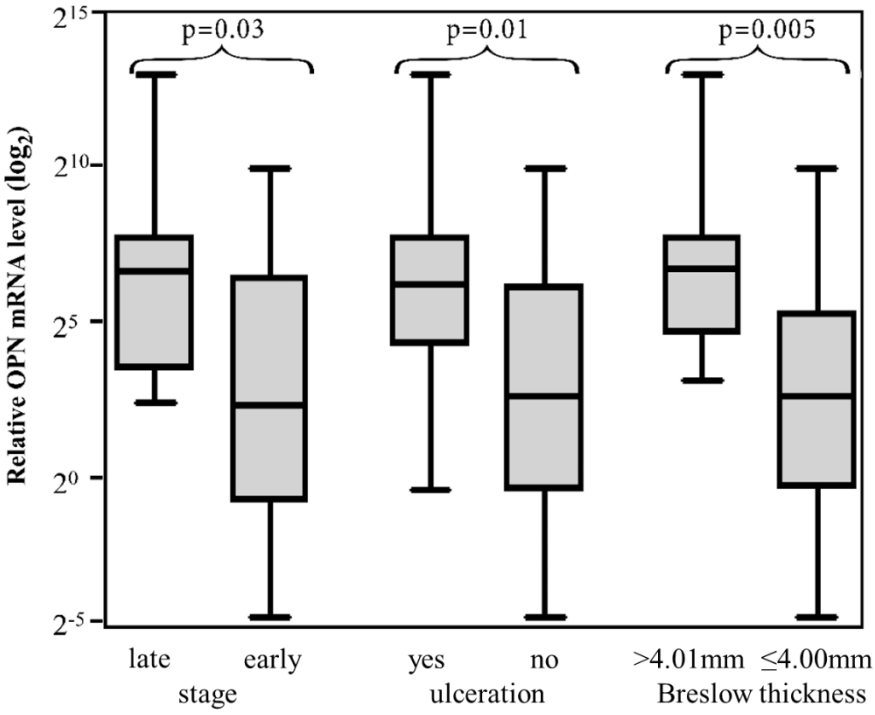

Figure 10. OPN mRNA levels in melanomas relative to control naevus. *Log_2-transformed data are displayed. Mann-Whitney-Wilcoxon exact test was used to reveal significant differences between the gene expression data and the clinical–pathological parameters of melanoma patients (N=28).*

In our study we were able to analyze both gene and protein expression levels in 14 of the examined samples, allowing the comparison between the gene and protein expression levels (**Table 5**). In the majority of primary melanoma samples, we detected elevated expression of the *OPN* gene which was associated with protein expression levels. Interestingly, our results revealed some inconsistencies where the proportion of osteopontin-expressing cells and the intensity of the antigen did not align with the high mRNA expression. For instance, sample 3 (characterized by poor prognosis) exhibited a high mRNA expression level but did not show high protein levels. When examining the relationship between OPN protein levels and mRNA expression, we did not observe any correlation. Several biological factors may influence this correlation, for one thing, translation of mRNA molecules is regulated by several mechanisms and regulatory processes and not all mRNA molecules are translated. On the other hand, the interactions between individual mRNA molecules and proteins may be different, leading to variation in correlation [110-112].

Table 5. Comparison of mRNA and protein expression levels of OPN in primary melanoma samples.

Tumour number	Relative mRNA level	Immunohistochemical score	
		Proportion	Staining intensity of the
1	20.33	3+	Strong
3	2926.14	1+	Weak
4	1.06	1+	Weak
5	2.90	2+	Weak
9	187.37	1+	Strong
11	36.69	3+	Strong
16	37.37	3+	Strong
17	14.02	3+	Strong
18	139.11	3+	Strong
19	0.80	3+	Weak
22	100.20	2+	Strong
25	5.30	0	None
26	865.76	2+	Weak
28	11.68	3+	Moderate

[a] The proportion score included the fraction of positively stained tumour cells as follows: 0=none, 1+ = <5 %, 2+ = 5–50 % and 3+ = >50 %

Association between OPN protein expression and clinical-pathological characteristics in primary melanomas

We studied OPN protein expression levels in 93 primary melanoma tissue samples. Positive OPN expression was detected in 81/93 (87%) primary tissues. The remaining 12 tumours were negative for OPN expression. Increased OPN protein level (2+ and 3+) were detected in 71% of primary melanoma samples. Melanoma tissues, in which at least the 50% of tumour cells exhibited high osteopontin expression, were categorized as 3+. High protein positivity (3+) was found in 40% of melanoma samples associated with unfavorable prognosis (ulcerated surface, nodular subtype, advanced stage, >4.01 mm Breslow thickness, presence of metastasis and <5-year survival). Examining the relationship between protein expression and the clinical-pathological characteristic of tumours, we found a statistically significant correlation with Breslow tumour thickness and presence of metastasis (p=0.021 and p=0.036, respectively **Table 6**). In general, we observed a lower percentage of tumour cells expressing the OPN protein in melanomas with a better prognosis (non-ulcerated surface, superficial spreading subtype, early stage, ≤4.00 mm thickness, non-metastatic tumours and >5-year survival).

Table 6. Correlation between OPN protein staining distributions of primary melanomas regarding clinical-pathological parameters.

Parameters	No. of tumours (%)	Staining category (%)				
		0	1+	2+	3+	p-value[a]
Subtype						0.091
SSM[b]	50 (53.8)	9 (18)	8 (16)	19 (38)	14 (28)	
NM[c]	43 (46.2)	3 (6.9)	7 (16.3)	11 (25.6)	22(51.2)	
Gender						1.000
Female	56 (60.2)	7 (12.5)	9 (16.1)	18 (32.1)	22(39.3)	
Male	37 (39.8)	5 (13.5)	6 (16.2)	12 (32.4)	14(37.8)	
Age						0.374
<50 years	23 (24.7)	3 (13)	4 (17.4)	10 (43.5)	6 (26.1)	
≥50 years	70 (75.3)	9 (12.9)	11 (15.7)	20 (28.6)	30(42.9)	
Breslow thickness						***0.021***
≤2.00 mm	36 (38.7)	7 (19.4)	6 (16.6)	15 (41.6)	8(22.2)	
2.01 – 4.00 mm	29 (31.2)	5 (17.2)	3 (10.3)	9 (31)	12(41.4)	
>4.01 mm	28 (30.1)	0 (0)	6 (21.4)	6 (21.4)	16(57.1)	
Clark's stage						0.155
I-III	48 (51.6)	9 (18.8)	8 (16.6)	17 (35.4)	14(29.2)	
IV-V	45 (48.4)	3 (6.6)	7 (15.5)	13 (28.8)	22(48.8)	
Ulceration						0.135
Absent	57 (61.3)	9 (15.8)	9 (15.8)	22 (38.6)	17(29.8)	
Present	36 (38.7)	3 (8.3)	6 (16.6)	8 (22.2)	19(52.7)	
Metastasis[d]						***0.036***
Absent	56 (60.2)	9 (16)	4 (7.1)	20 (35.7)	23(41)	
Present	37 (39.8)	3 (8.1)	11 (29.7)	10 (27)	13(35.1)	
Patient's survival[e]						0.145
Alive	54 (58)	9 (16.6)	5 (9.3)	19 (35.2)	21(38.8)	
Exitus	39 (42)	3 (7.7)	10 (25.6)	11 (28.2)	15(38.5)	

Significant *p* values are indicated in italic.
[a]Two-sided Fisher's exact test; [b]Superficial spreading melanoma; [c]Nodular melanoma; [d]Metastasis of the examined primary tumours; [e]Patients with at least 5-year follow-up period were included.

Since some tumour cells may exhibit varying levels of protein expression, we also accessed the intensity of protein expression. According to our results, we found that melanoma samples with poor clinical outcome showed stronger OPN staining. We analyzed the association between the OPN expression levels and clinical-pathological parameters of the primary tumours. **Figure 11** shows the result of our analysis. It is noticeable, that increased OPN expression was significantly associated with increasing tumour Breslow thickness (*p=0.007*, proportion of tumour cells and Breslow thickness; *p*=0.033, staining intensity and Breslow thickness).

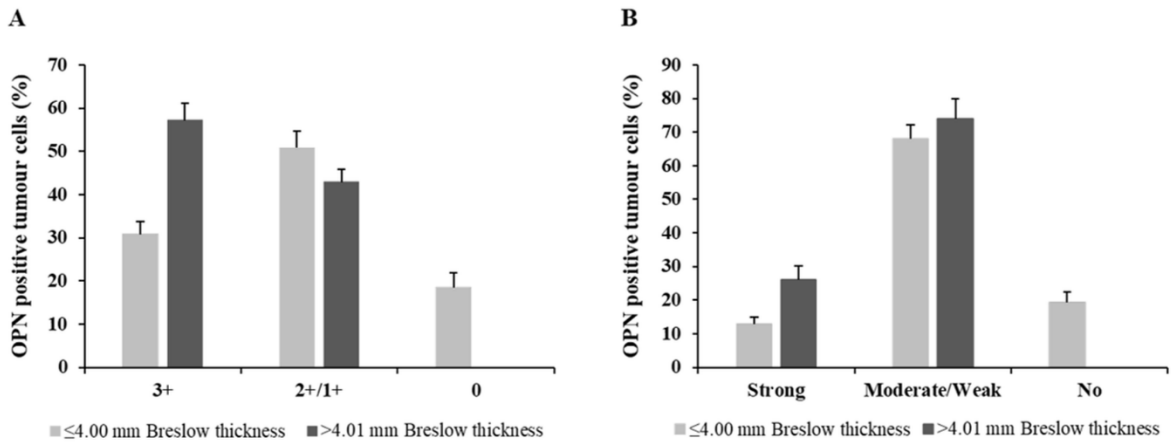

Figure 11. Relationship between the Breslow thickness of primary melanomas (N=93) and the OPN positive tumour cells. *(A) Proportion of positively stained tumour cells (p=0.007; Fisher's exact test) and (B) their staining intensity (p=0.033; Fisher's exact test).*

Multivariate logistic regression analysis was used to investigate the effect of OPN expression and prognostic factors on metastasis formation. We found a 1.39-fold increased risk of metastasis in OPN expressing melanomas, but this association did not reach statistical significance (*p*=0.691). Furthermore, we found that patients with primary tumours exceeding 4.00 mm in thickness (*p*=0.032) and those with ulcerated surface (*p*=0.002) were significantly more likely to develop metastasis (**Table 7**).

Table 7. Logistic regression analysis of the impact of various prognostic factors on metastasis formation.

Variables	Odds ratio	CI[a]	*p* value
Breslow thickness	**3.11**	**1.10-8.75**	***0.032***
Clark level	0.49	0.12-2.14	0.348
Osteopontin score (1, 2 and 3 vs 0)	1.39	0.27-7.15	0.691
Ulceration	**5.47**	**1.85-16.17**	***0.002***

Significant *p* values are indicated in italic.
[a]Confidence interval (95%).

We examined the association between OPN expression levels, various prognostic factors and survival using multivariate Cox regression analysis. In this study, we demonstrated that high OPN expression (staining score of 2 or 3) [hazard ratio (HR)=2.02, 95% confidence interval (CI)=0.99-4.14; p=0.050], tumour thickness [HR=1.66, 95% CI=1.01-2.74, p=0.046] and the presence of metastasis [HR=14.25, 95% CI=4.98-40.77, p<0.001] were significantly associated with reduced survival of melanoma patient.

OPN gene expression in melanoma

To identify mRNA expression changes related to melanoma progression *in vitro,* qRT-PCR were performed on primary melanoma (n=12) and melanoma metastases (n=8) originated cell lines. Comparison of the gene expression data of the primary tumour originated and metastatic tumour originated cell lines, we found that the relative *OPN* mRNA expression significantly higher in the cell lines derived from the melanoma metastasis*(p=0.04)* (**Figure 12**).

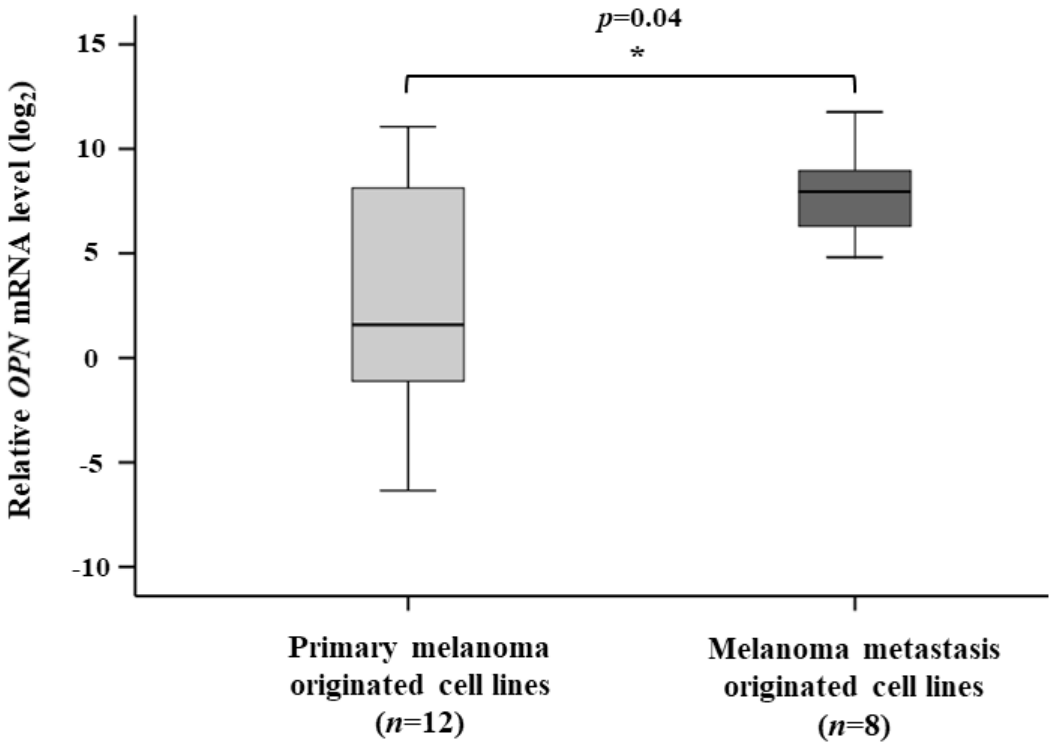

Figure 12. Comparison of the relative OPN mRNA expression in primary melanoma originated- and melanoma metastasis originated cell lines. *The data are presented as the means (± SD) of three replicates/samples. The asterisk indicates statistically significant difference ($p \leq 0.05$; Mann-Whitney test).*

We also aimed to compare the relative OPN expression associated with the $BRAF^{V600E}$ and *NRAS* mutation statuses of the cell lines. The overall frequency of the $BRAF^{V600E}$ mutation was 70%, while the *NRAS* mutations (20%) were less frequent in our melanoma cell line panel, and none of the cell lines exhibited both mutations at the same time. Mutation statuses of the cell lines are shown in **Table 4**. According to the gene expression results, cell lines with $BRAF^{V600E}$ mutation (n=14) exhibited significantly higher mRNA expression of the *OPN* gene compared to cell lines with wild-type *BRAF* mutation (n=6) (see **Figure 13**).

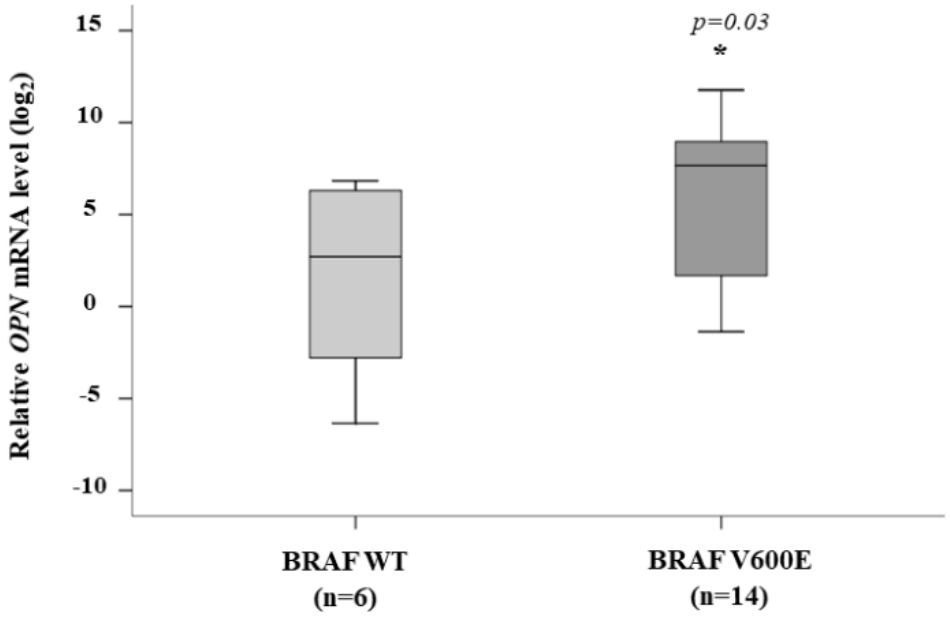

Figure 13. Relative gene expression of OPN in BRAF^{V600E} mutant and BRAF wild-type primary and metastatic melanoma cell lines. *Significantly higher expression of OPN mRNA was observed in cells with BRAF mutation compared to wild-type BRAF cells ($p \leq 0.05$; Mann-Whitney test). The data are presented as the means (± SD) of three replicates/samples. Asterisk represent significant difference between the two groups.*

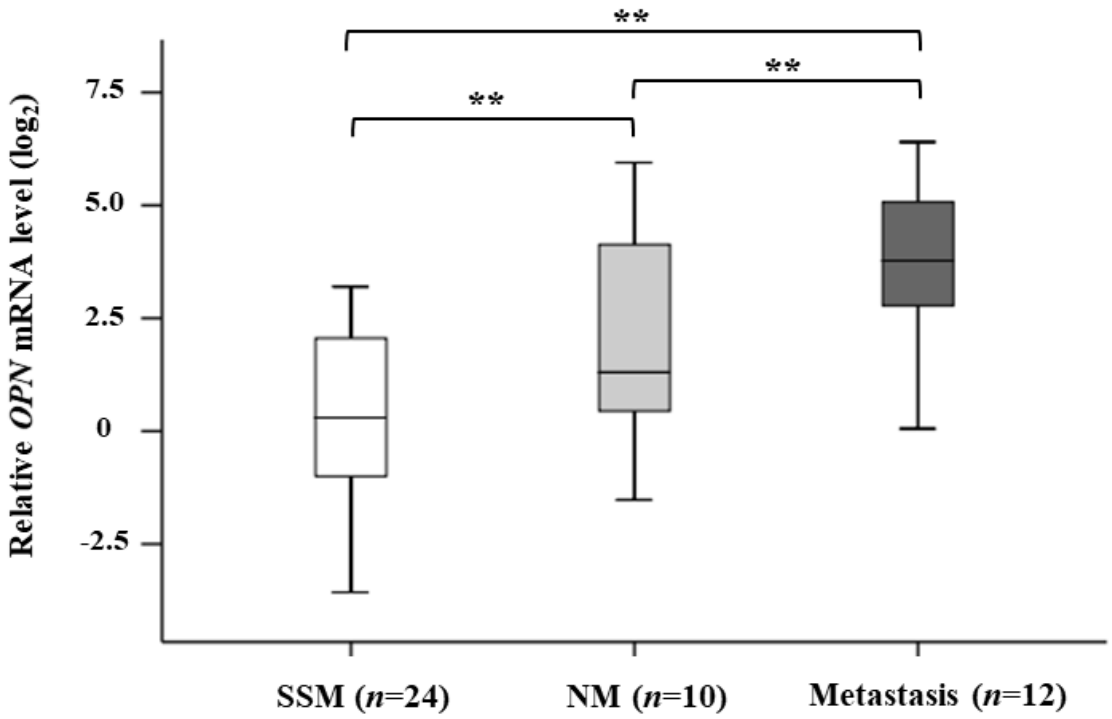

Figure 14. Relative OPN gene expression in different subtypes of melanoma tissue samples. *Box-plot represent the results of qRT-PCR analysis. Data displayed as means ± SD of three independent experiments. The asterisk indicates statistically significant difference ($p \leq 0.001$; Kruskal-Wallis test). SSM: superficial spreading melanoma; NM: nodular melanoma.*

We also analyzed the relative mRNA expression of the *OPN* in primary and metastatic tumour tissues. The clinical-pathological parameters of the tumours are summarized in **Table 3**. Our data showed significant differences between melanoma subgroups (p=0.0005; Kruskal-Wallis test) (**Figure 14**). We observed the highest relative gene expression in a melanoma metastasis (84.5). For 8 of the 12 metastatic samples the range was between 13.1-84.5. In the group of aggressive nodular subtypes (n=10), three primary tumours also showed elevated relative OPN expression (17.6-61.8), while samples from the less aggressive superficial spreading subtypes (n=24) exhibited a more uniform pattern with low *OPN* gene expression (range between 0.1-9.14).

OPN gene expression and NF-κβ p65 protein level in melanoma cell lines

As nuclear factor-κβ (NF-κβ) has the ability to activate OPN expression in cancer cells, this analysis aimed to determine the subcellular distribution of both OPN and NF-κB p65 protein. The staining and localization patterns were visualized and examined using confocal microscopy, allowing us to gain insights into the intracellular localization and potential interaction between OPN and NF-κβ p65. **Figure 15** illustrate the localization of OPN and the NF-κβ p65 proteins in selected cell lines (WM35 and WM278). This figure provides visual representations of the intracellular distribution and co-localization patterns of OPN and NF-κβ p65 proteins in these cell lines. The images captured using immunofluorescence labeling and confocal microscopy highlight the subcellular compartments where OPN and NF-κB p65 are localized, offering insights into their potential interactions and functional relevance within the studied cell lines. In the WM35 cell line, which originated from early lesion of a primary tumour (RGP, SSM subtype) without metastatic potential, the expression of OPN and NF-κB p65 protein was observed in the cytoplasm (**Figure 15A and 15C**).

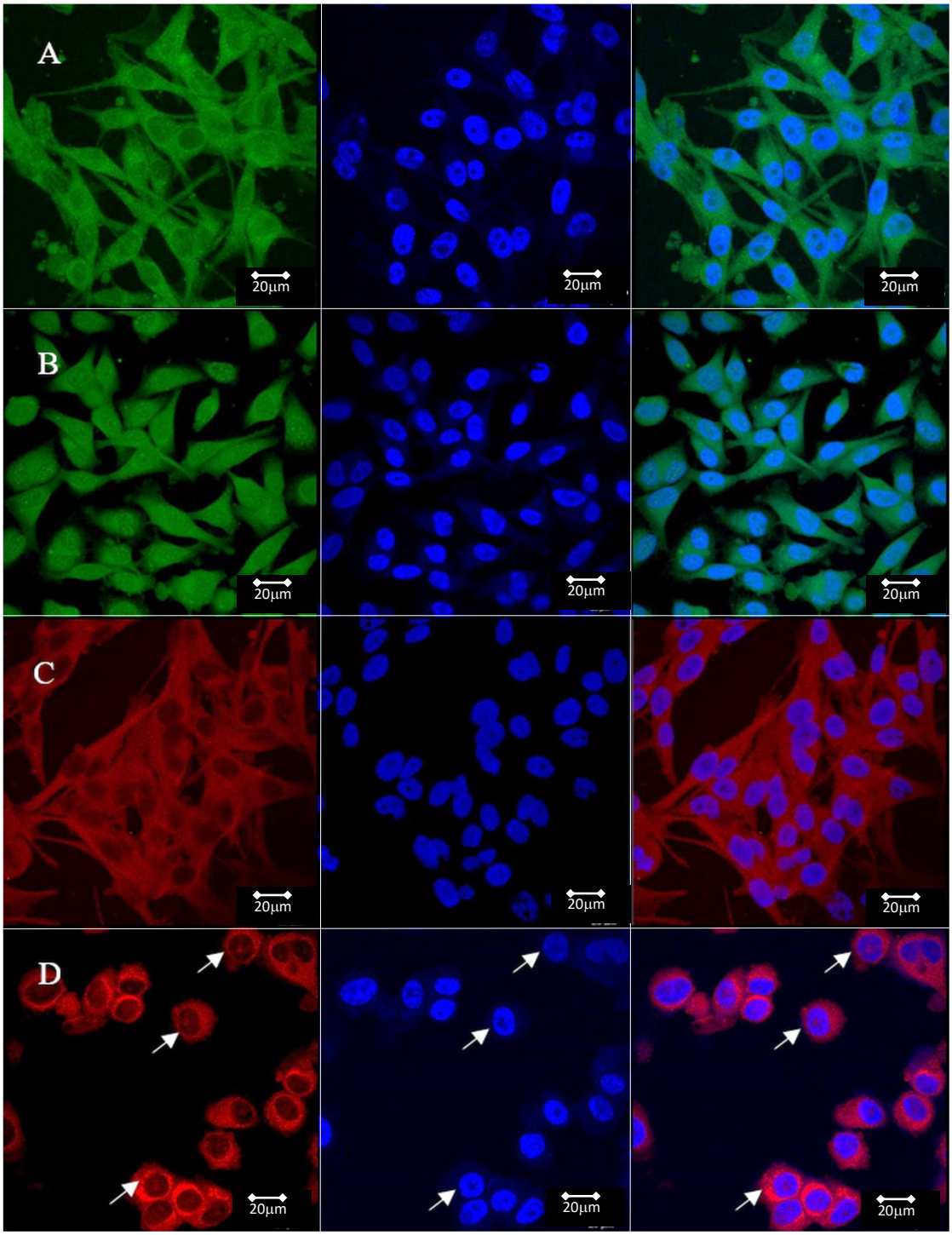

Figure 15. Confocal laser scanning images of OPN and NF-κβ p65 proteins localisation in melanoma cell lines. *OPN protein expression (green fluorescence) in melanoma cell lines: WM35 (A) and WM278 (B). NF-κβ p65 protein (red fluorescence) - mainly cytoplasmic staining is present in the WM35 cells (C), whereas both cytoplasmic and spotted nuclear staining can be observed for the NF-κβ p65 protein in the WM278 cells (D). Nuclei are stained with DAPI (blue). Arrows represent cells with nuclear translocation for the NF-κβ p65 protein. DyLight594 (red fluorescence) anti-rabbit secondary antibody was used. DAPI was applied to stain nuclei (blue fluorescence). Scale bars represent 20 µm.*

On the other hand, in the WM278 which is a tumorigenic primary melanoma cell line (VGP, NM subtype) with competence for metastasis, expression of both OPN and NF-κβ p65 protein was observed in both the cytoplasm and nuclei (**Figure 15B and 15D**). Z-stack images of the labelled NF-κβ p65 protein were recorded for WM278 cells. The Z-stack images collected from 0.4-µm sections are shown in the top left panel of the figure. The section depth of the cell sections is identified at the top left of each image (**Figure 16**), and the magnification of each cell section is displayed in the bottom right corner of the images (scale bar, 10 µm). The **a** and **b** of the top right panel of **Figure 16** show consecutive optical slices through a cell and generating orthogonal projections of all slices in a Z-series.

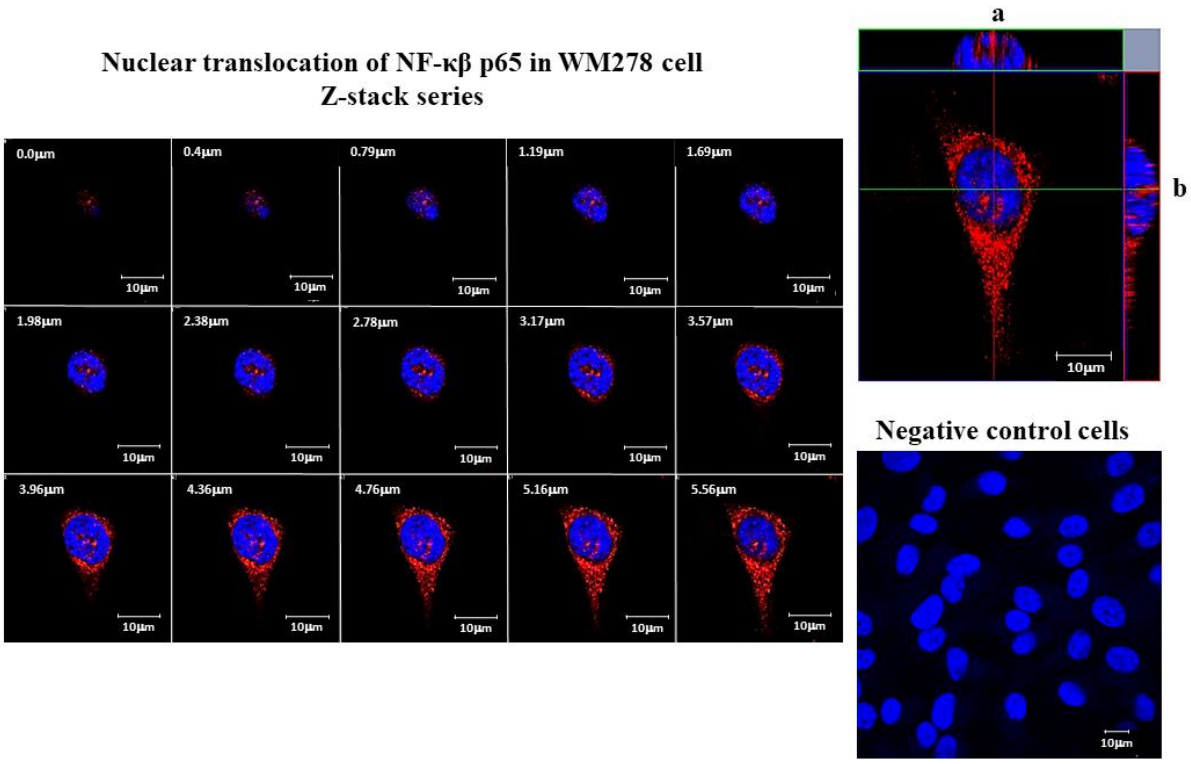

Figure 16. Confocal microscopy Z-stack imaging showing NF-κβ p65 localization within WM278 cell nuclei.

The data clearly demonstrate that NF-κβ p65 is localized in the nucleus. OPN protein expression in the cell lines was similar to that of the NF-κβ p65 protein, which is the main target of OPN signaling.

Effect of RNAi on OPN expression

In order to determine the effectiveness of OPN-siRNA silencing, we chose a primary and metastatic cell line pair (WM278 – WM1617) that were originated from the same patient. Both cell lines had $BRAF^{V600E}$ mutation and were wild type for *RAS* gene. We effectively inhibited OPN expression in melanoma cell lines with high OPN expression using validated OPN-specific siRNA. In our experiments, we used AllStars Negative Control siRNA (NC-siRNA) as a negative control. To investigate the potential impact of OPN silencing on gene expression, we carried out real time PCR experiments and quantified the relative mRNA level of *OPN* gene. According to our results, siRNA-mediated *OPN* knockdown in melanoma cell lines resulted in an average 60% inhibition rate of *OPN* mRNA levels compared to the negative control. **Figure 17A** demonstrates the significant decrease in the relative *OPN* gene expression in primary tumour- and metastasis-derived melanoma cell lines ($p \leq 0.05$). At the same time, the proliferation of the transfected cells was significantly reduced compared to the NC-siRNA treated and untreated control cells (**Figure 17B**).

For the selected primary and metastatic cell line pairs, we also investigated the possible changes in OPN protein expression in response to silencing using Proteome Profiler Oncology Array. Similarly, to the change in gene expression, the significant decrease in OPN protein expression was observed in both cell lines (**Figure 17C**).

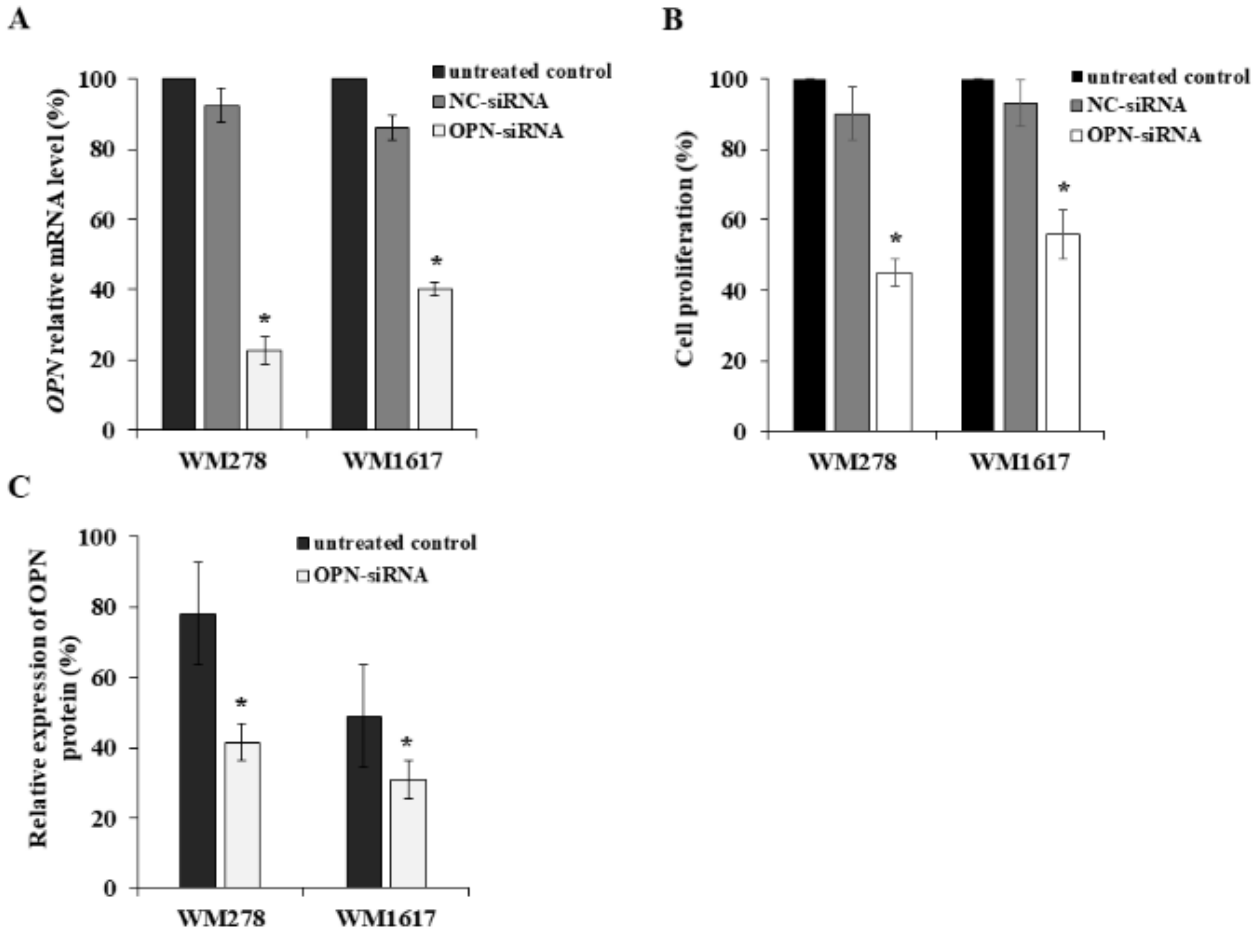

Figure 17. OPN-siRNA inhibition of the relative gene expression of OPN in melanoma cell lines*. (A) Relative gene expression of OPN after transfection using 5 nM AllStars Negative Control siRNA (NC-siRNA) and OPN-specific siRNA. (*p≤0.05; Mann-Whitney test). (B) The proliferation of untreated, NC-siRNA and OPN-siRNA treated melanoma cell lines. (*p≤0.005; Student's t-test). (C) Changes in OPN protein expression in untreated and OPN-siRNA treated cell lines. (*p≤0.05; Student's t-test). The data for each cell lines are presented as the means ± SD of three independent experiments*.

Effect of RNAi on the invasive behaviour of melanoma cell

In order to identify the invasive potential of OPN-siRNA silenced cells, invasion assay was performed after OPN knockdown. During these experiments, we selected a primary melanoma originated cell line with high OPN expression (WM278). Based on the invasion assay, we observed that silencing the OPN resulted in a significant reduction of the invasive potential in the WM278 cells. **Figure 18A** clearly shows the difference between the invaded cells: on

average 91 (±16) control cells/field invaded onto the membrane surface, while only 49 (±10) OPN-siRNA transfected cells. We found that invasion was significantly lower in silenced cells compared to control cells, suggesting that downregulated OPN expression is associated with reduced invasion (**Figure 18B**). The reduced *OPN* expression was confirmed using real-time quantitative PCR (**Figure 18C**).

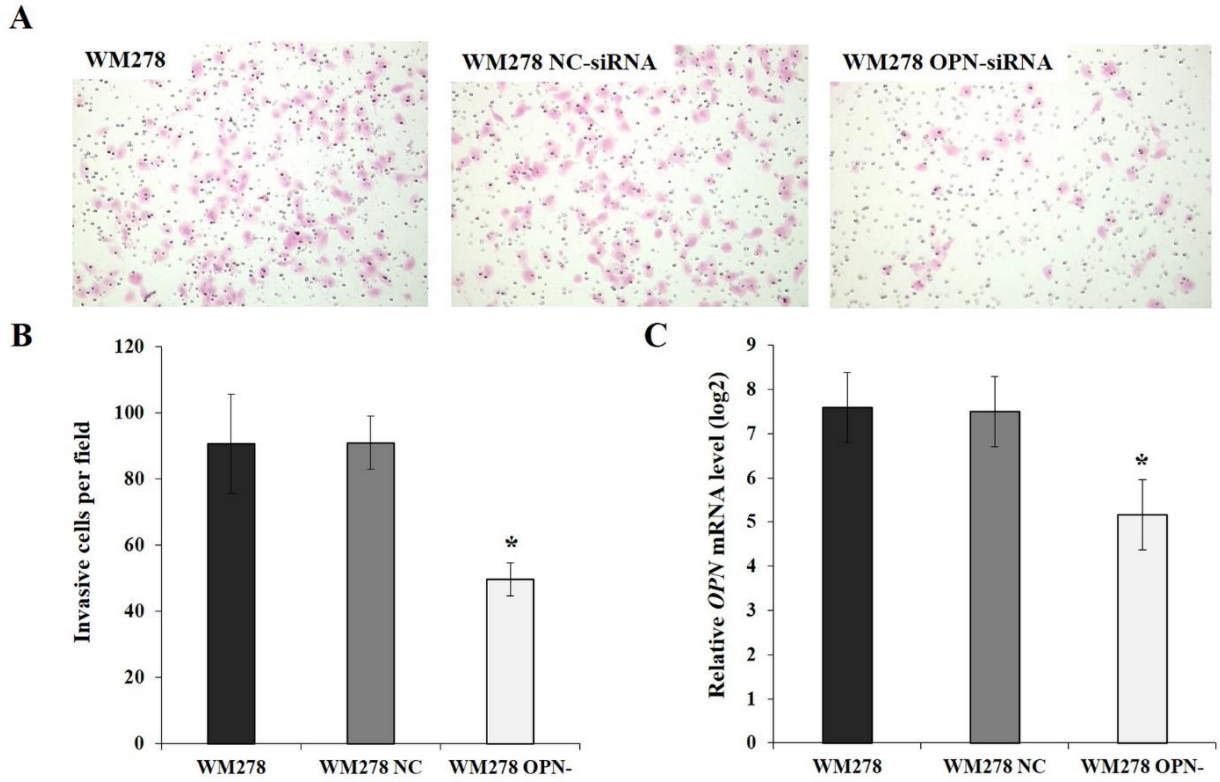

Figure 18. Invasive potential of primary tumour derived WM278 cell line. *(A) Representative images of cell invasion of WM278 cell line. Cells were cultured in Matrigel invasion chambers for 24h. The invaded cells on the lower layer were fixed with methanol and stained with haematoxylin–eosin (200X magnification). (B) Quantification of the invasion assays. The invaded cells were counted in seven randomly selected microscopic fields on the membrane and the results are summarized and expressed as the mean number of invaded cells. (C) Quantitative measurement of OPN mRNA level in WM278 cells. The data are presented as the mean ± SD of three independent experiments. Asterisk indicates significant difference between the control and OPN silenced cell lines. ($p \leq 0.05$; Student's t-test) Black column: untreated cells; grey column: Negative Control siRNA (NC-siRNA) transfected cells; white column: OPN-siRNA transfected cells).*

Protein array analysis of the original and OPN siRNA-transfected cells

We also aimed to determine protein expression differences between the original and OPN siRNA-transfected cell lines, we used a Proteome Profiler Human XL Oncology Array, that includes 84 cancer-related proteins. Considerable changes in the expression levels of several proteins were observed. The list of the proteins, as well as the relative protein expressions of the melanoma cell lines are summarized in **Supplementary Table 1**. Out of the 84 proteins examined, 26 proteins were expressed in the primary tumour originated WM278 melanoma cell line, whereas three proteins in the metastasis originated WM1617 cell line. In these two cell lines, we performed silencing of the osteopontin gene using OPN-specific siRNA. We found that 19 proteins expressed in the primary tumour derived OPN siRNA silenced WM278 cell line, while 37 proteins expression were detected in the metastasis derived transfected WM1617 cells. A number of differentially expressed proteins were found between the original and transfected cell lines (**Figure 19**). When comparing the protein expression between the original and transfected WM278 cell lines, we observed that out of the 26 proteins expressed in the original cell lines, 9 proteins showed no detectable expression (indicated with blue numbers on **Figure 19**), 15 proteins had lower expression (indicated by red numbers), and 3 proteins exhibited higher (indicated by green numbers) expression. In the case of the comparison between the protein expression patterns of the original and transfected WM1617 cell lines, we found that 37 proteins were expressed in the transfected variants. The majority of the proteins (n=19, indicated by green numbers) showed lower expression level in the siRNA transfected cells compared to the original WM1617 cells, while 15 proteins (indicated by red numbers) had higher expression. Additionally, three proteins expressed in the WM278 cell line showed no expression. Notably, the expression of OPN was consistent in both cell lines, WM278 and WM1617, the protein expression decreased in both siRNA silenced cell lines.

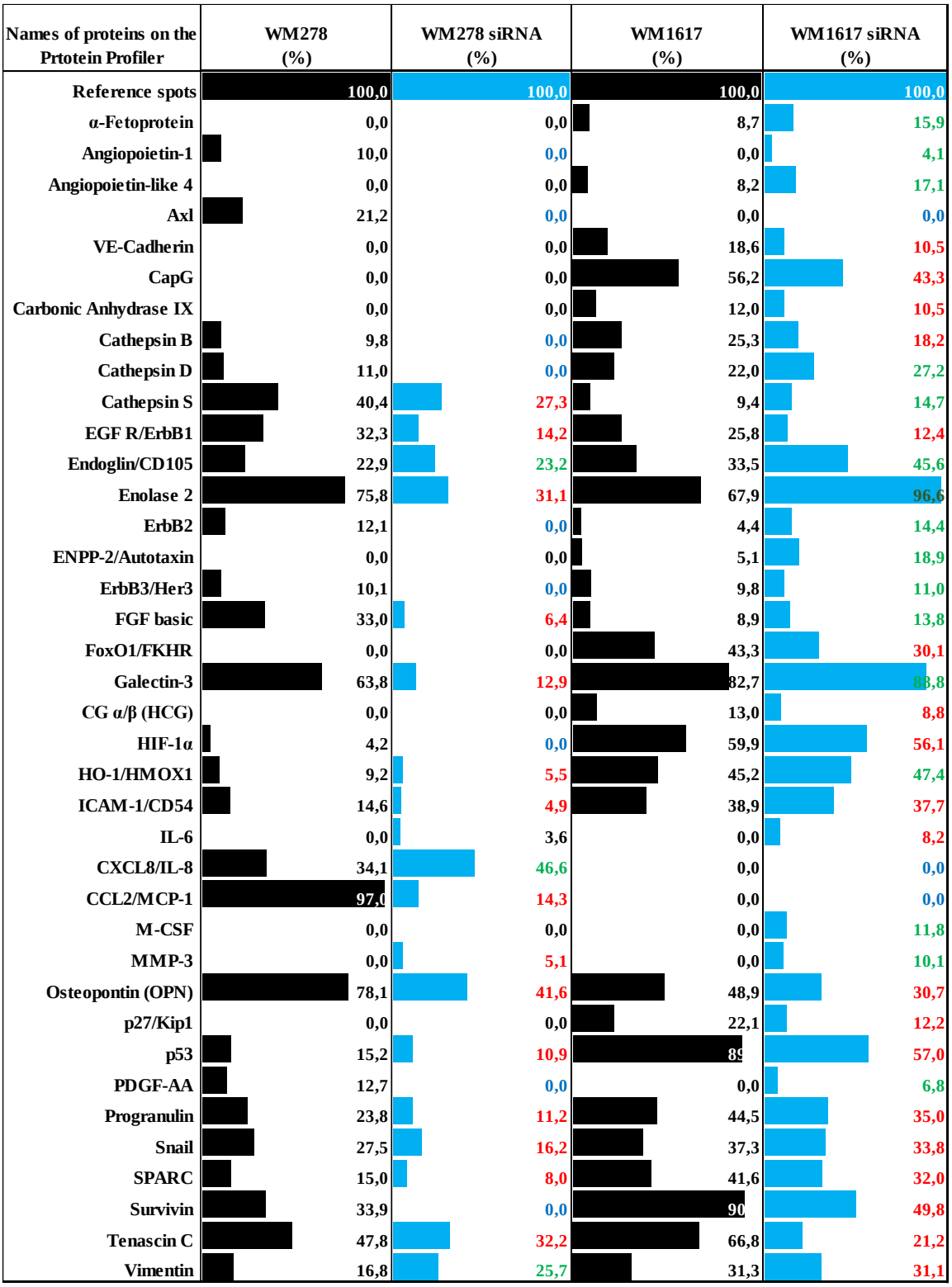

Names of proteins on the Prtotein Profiler	WM278 (%)	WM278 siRNA (%)	WM1617 (%)	WM1617 siRNA (%)
Reference spots	100,0	100,0	100,0	100,0
α-Fetoprotein	0,0	0,0	8,7	15,9
Angiopoietin-1	10,0	0,0	0,0	4,1
Angiopoietin-like 4	0,0	0,0	8,2	17,1
Axl	21,2	0,0	0,0	0,0
VE-Cadherin	0,0	0,0	18,6	10,5
CapG	0,0	0,0	56,2	43,3
Carbonic Anhydrase IX	0,0	0,0	12,0	10,5
Cathepsin B	9,8	0,0	25,3	18,2
Cathepsin D	11,0	0,0	22,0	27,2
Cathepsin S	40,4	27,3	9,4	14,7
EGF R/ErbB1	32,3	14,2	25,8	12,4
Endoglin/CD105	22,9	23,2	33,5	45,6
Enolase 2	75,8	31,1	67,9	96,6
ErbB2	12,1	0,0	4,4	14,4
ENPP-2/Autotaxin	0,0	0,0	5,1	18,9
ErbB3/Her3	10,1	0,0	9,8	11,0
FGF basic	33,0	6,4	8,9	13,8
FoxO1/FKHR	0,0	0,0	43,3	30,1
Galectin-3	63,8	12,9	82,7	88,8
CG α/β (HCG)	0,0	0,0	13,0	8,8
HIF-1α	4,2	0,0	59,9	56,1
HO-1/HMOX1	9,2	5,5	45,2	47,4
ICAM-1/CD54	14,6	4,9	38,9	37,7
IL-6	0,0	3,6	0,0	8,2
CXCL8/IL-8	34,1	46,6	0,0	0,0
CCL2/MCP-1	97,0	14,3	0,0	0,0
M-CSF	0,0	0,0	0,0	11,8
MMP-3	0,0	5,1	0,0	10,1
Osteopontin (OPN)	78,1	41,6	48,9	30,7
p27/Kip1	0,0	0,0	22,1	12,2
p53	15,2	10,9	89	57,0
PDGF-AA	12,7	0,0	0,0	6,8
Progranulin	23,8	11,2	44,5	35,0
Snail	27,5	16,2	37,3	33,8
SPARC	15,0	8,0	41,6	32,0
Survivin	33,9	0,0	90	49,8
Tenascin C	47,8	32,2	66,8	21,2
Vimentin	16,8	25,7	31,3	31,1

Figure 19. Changes in relative protein expression in original (WM278 and WM1617) and OPN-siRNA transfected melanoma cell lines (WM278 OPN-siRNA and WM1617 OPN-siRNA). *Expression results were obtained by Proteome Profiler Human XL Oncology Array Kit. The intensity of the reference is displayed as 100%. Numbers in the columns indicate the protein expression as a percentage of the intensity of the reference spots on the array. Green numbers indicate decreased, red numbers indicate increased and blue numbers indicate no expression if the certain protein.*

Importantly, beside OPN, altered expression of five proteins (EGFR, tenascin C, survivin, galectin-3 and enolase 2) was detected collectively in both transfected cell lines. In addition to OPN, we found decreased expression of five proteins (EGFR, tenascin C, survivin, galectin-3 and enolase 2) in the WM278^{OPN-} cell line. Interestingly, WM1617^{OPN-} cells, which are the metastatic pair of WM278 cells, showed a different pattern. Decreased expression of four proteins (OPN, EGFR, tenascin C and survivin) was verified in the silenced metastatic cell line, whereas enhanced expression of the two other proteins was found (galectin-3 and enolase 2) (**Figure 20**).

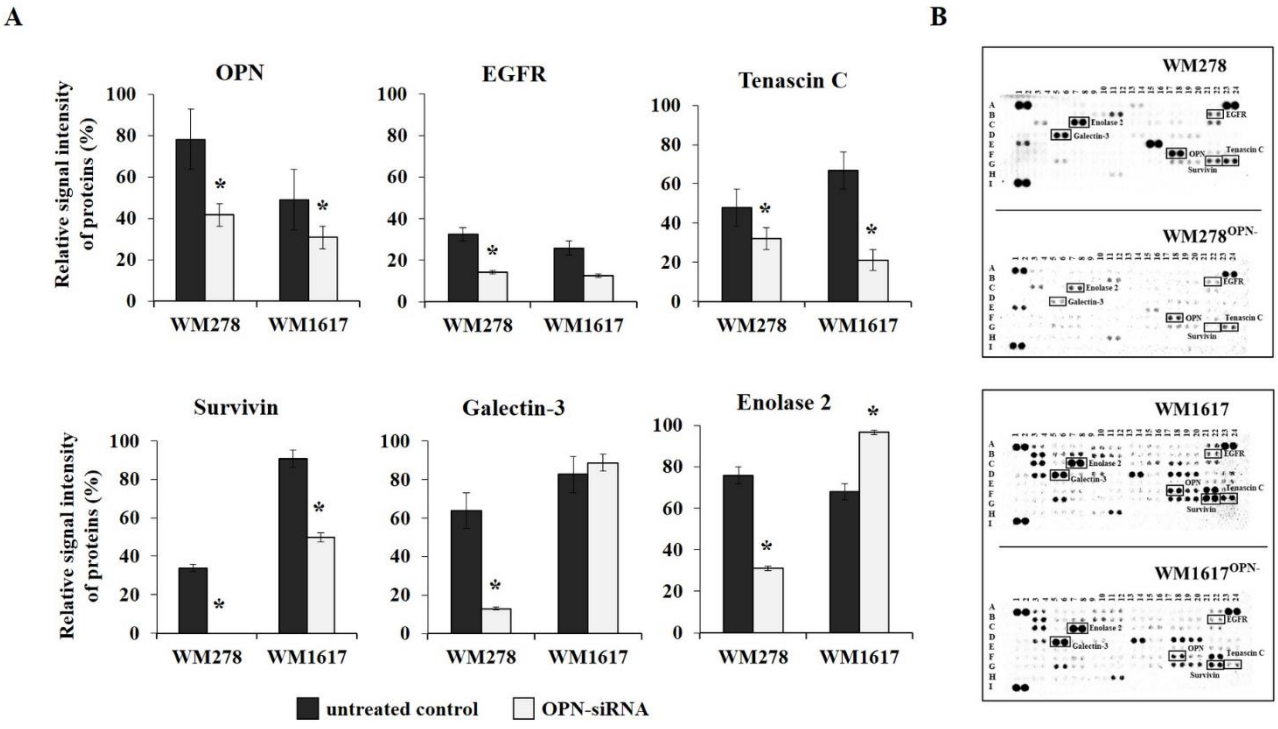

Figure 20. Relative expression of six proteins (OPN, EGFR, tenascin C, survivin, galectin-3 and enolase 2) in untreated (WM278 and WM1617) and in transfected melanoma cell lines (WM278 OPN-siRNA and WM1617 OPN-siRNA). *(A) The graph displays the relative intensity of the proteins. The data are presented as the mean ± standard deviation (SD) with three replicates per sample. Asterisks represent significant differences ($p \leq 0.05$; Student's t-test). Black columns: untreated control cells; grey columns: OPN-siRNA silenced cells. (B) Representative image of proteome profile analysis (Proteome Profiler Human XL Oncology Array membrane image). Black squared dots indicate the localization and expression of six proteins that exhibited common expression changes in transfected cell lines.*

In order to validate the proteome profiler data, we also performed gene expression analysis by real time quantitative PCR method for the examined cell lines. We found that the data are consistent with the protein array results. Therefore, the gene expression pattern of the six genes (*OPN, EGFR, tenascin C, survivin, galectin-3 and enolase 2*) changed in the same direction as observed in the Proteome Profiler array (**Figure 21**).

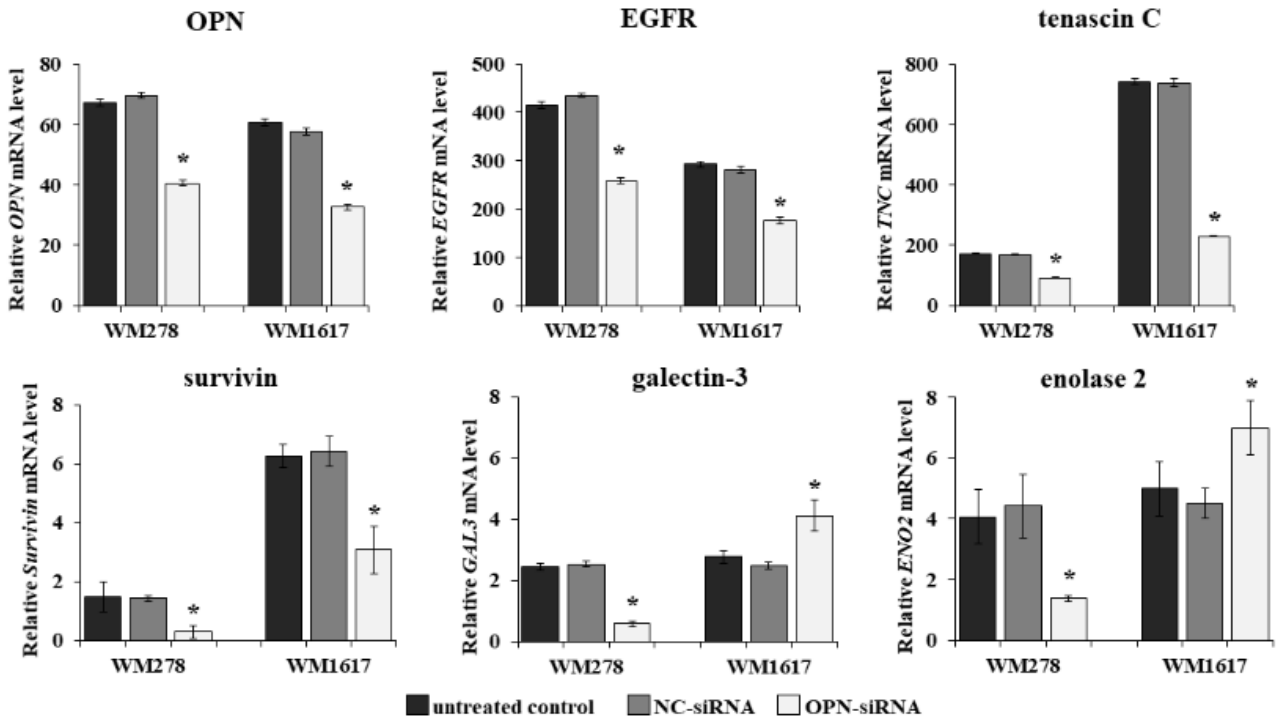

Figure 21. Relative expressions of six genes (OPN, EGFR, tenascin C, survivin galectin-3 and enolase 2) in the parental cells and OPN-siRNA silences melanoma cells. *Data are presented as the mean ± standard deviation (SD) with three replicates per sample. Significant changes in proteins expression after OPN silencing (p≤0.05; Mann-Whitney test) are labelled with asterisks (*).*

Proteins and their functional interactions are at the centre of the framework of cellular function. To fully understand biological processes, their relationships must be taken into account. In our study, we used the Search Tool for the Retrieval of Interacting Genes (STRING) (*http://string-*

db.org) analysis for differentially expressed proteins to predict protein-protein interaction network associated with functional pathways. The STRING database is designed to collect, refine and integrate all publicly available sources on protein-protein interactions and supplement them with predictions. As illustrated on **Figure 22**, original (WM278 and WM1617) and OPN-siRNA silenced (WM278 OPN-siRNA and WM1617 OPN-siRNA) cell lines showed a differential protein interaction with a high confidence level 0.700.

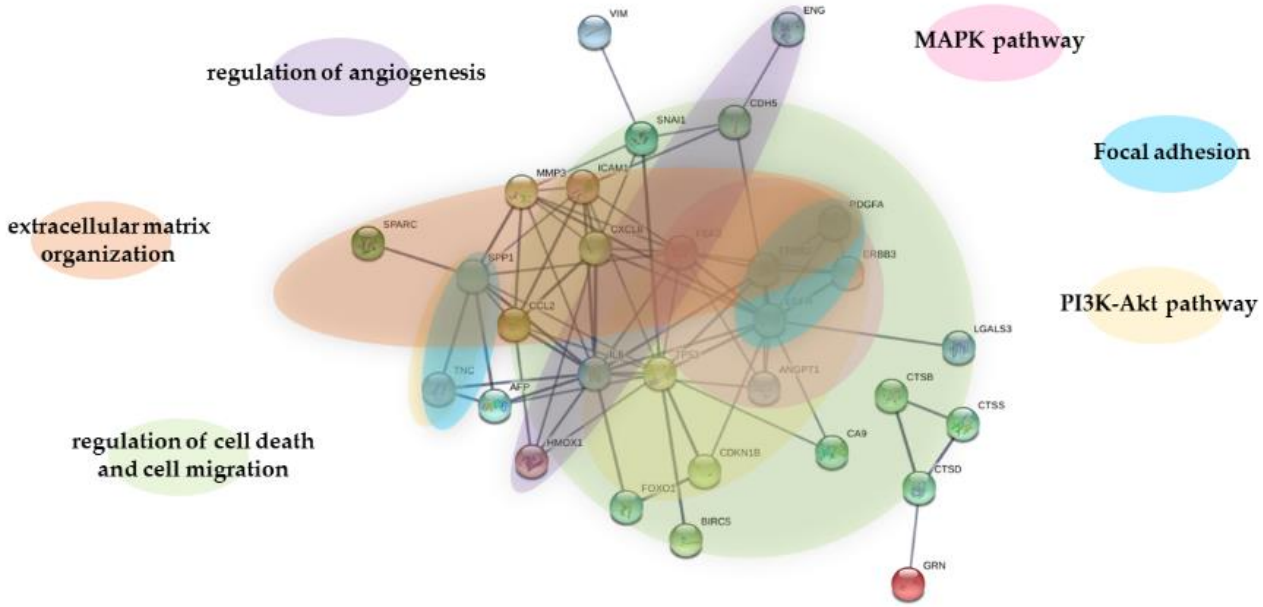

Figure 22. Protein-protein interaction network was constructed using the STRING analysis of WM278 and WM1617 cells. *We utilized database version 11.0 to identify the protein-protein interactions among the 38 proteins that exhibited differential expression in original and silenced cell lines. Only interactions with a high confidence level (0.700) were considered for the analysis, while proteins with no predicted interactions were excluded.*

Multiple clusters of proteins were formed, one cluster for extracellular matrix organization, another cluster for the regulation of angiogenesis, cell death and cell migration, and the last cluster for PI3K-Akt, MAPK and focal adhesion signaling pathway.

Discussion

It is clearly demonstrated that OPN involved in various aspects of cancer biology, including cell adhesion, migration, invasion and angiogenesis [16, 64, 113]. The expression of this protein can influence the tumour microenvironment and modulate the immune response. Recently, OPN has been studied extensively as a potential biomarker for the detection of metastatic tumours. Various investigations have demonstrated that elevated levels of the OPN protein are often found in the peripheral blood of patients with metastatic tumours [65]. OPN has gained significant attention as a possible diagnostic and prognostic biomarker in various types of cancer. Maier and colleagues have successfully increased the sensitivity and specificity of melanoma metastasis prediction by combining plasma OPN levels with the protein marker S100 [114]. The detection of metastatic tumours at an early stage is crucial for effective treatment and improved patient outcomes. Biomarkers like OPN provide valuable information to clinicians, helping them diagnose the presence of cancer, determine its stage, and monitor the effectiveness of treatment. Research in the field of oncology continues to explore the potential of OPN and other biomarkers to enhance cancer diagnosis and management [16, 19, 115].

The aim of our study was to understand the molecular mechanism of OPN expression during melanoma progression. Studying the specific molecular mechanisms involved during the progression of melanoma, can provide crucial insights into the diagnosis and treatment of the disease. Understanding these mechanisms may lead to the development of targeted therapies that can specifically inhibit or modulate OPN, thereby potentially slowing down or preventing the development of melanoma metastasis. It could pave the way for personalized treatment strategies, improving the overall prognosis and quality of life for individuals affected by melanoma.

Our research group using a high throughput Affymetrix gene expression array found that OPN had the highest expression levels in melanoma tissue samples which was associated with less

favourable clinical outcome [15]. Therefore, our first objective was to validate these microarray results using qRT-PCR. During our analysis, we observed that increased *OPN* mRNA levels was significantly associated with advanced stages of melanomas (Clark IV-V), ulcerated surface, and greater thickness (more than 4 mm). These observations indicate a potential role of OPN in melanoma progression and aggressiveness.

In order to further investigate the protein levels of OPN, we extended our studies and created tissue microarray platforms consisting of 93 primary melanoma tissues. Through immunohistochemistry analysis performed on these primary melanoma samples, we observed elevated level of OPN protein, which was associated with poor prognosis. While, our protein and gene expression results did not demonstrate a clear relationship in all samples, on average, we found that the high levels of *OPN* mRNA were correlated with strong antigen positivity. It is important to note that the relatively limited number of melanoma specimens may be one of the reason for this phenomenon. Furthermore, variations in the interactions between individual mRNA molecules and proteins can lead to differences in correlation. The lifetime and degradation rate of mRNA may be variable and not all mRNA molecules are translated [110-112]. In melanoma, the significant heterogeneity within tumour tissues may also influence the differences between mRNA and protein levels. Due to both inter-tumoral and intra-tumoral heterogeneity, the genetic profile of individual patients can vary considerably and this genetic diversity can influence mRNA expression and protein synthesis. Aberrations in molecular and signaling pathways are common in melanoma cells, and these alterations can subsequently affect mRNA and protein levels [116, 117]. Furthermore, epigenetic changes, including methylation and histone modifications, can also influence the regulation of mRNA and protein expression [118]. The interplay of these factors creates ambiguity in the relationship between mRNA and protein levels. Achieving a more precise and comprehensive understanding of the relationship requires complex experiments and analyses.

Our study also aimed to investigate the impact of OPN expression and prognostic factors on metastasis formation. We discovered a metastasis formation is more characteristic on primary melanomas with greater Breslow thickness. Additionally, we observed that high OPN expression served as a predictor of survival after considering thickness and metastasis formation. Patients with high OPN expression (score of 2 or 3) had a 2.02-fold higher risk of death from disease (p=0.050). Elevated OPN expression has been associated with advanced stage, tumour invasion and metastasis in various types of cancers. Previous studies demonstrated that OPN functions in versatile manner, involving the induction of multiple signaling pathways (PI 3'-kinase/Akt, NF-kB) through integrin and CD44 receptors which play a role in mediating metastatic processes [119-121]. Previously, published data support the notion that OPN binding to integrin activates the phosphorylation cascade of the NF-κβ pathway, leading to increased nuclear translocation of the p50 and p65 subunits of NF-κβ [19, 122-124]. This activation promotes various cellular processes, including cell proliferation, survival, angiogenesis, tumour growth and developing metastasis [125, 126]. By employing immunohistochemistry, we observed nuclear translocation of the NF-κβ p65 protein in the melanoma cell line (WM278), which exhibited high *OPN* mRNA expression. This finding, suggest that OPN induces activation of the NF-κβ pathway activation, aligning with previously published research [19, 127]. Conversely, melanoma cell lines with low OPN expression did not display NF-κβ p65 nuclear localization. This result strongly supports the hypothesis that the integrin-binding domain of OPN plays a crucial for in melanoma metastasis formation.

In the last decade, RNAi, a post-transcriptional mechanism for inhibiting gene expression, has demonstrated promising results in molecular-targeted gene therapy for various types of cancer [128, 129]. Knockdown of OPN has shown antimetastatic and antitumorigenic effects in diverse cancers [130-133], but, limited data are available for malignant melanoma [22, 134]. Therefore, in this study, our objective was to inhibit osteopontin expression using RNAi in

selected cell lines, characterized with high OPN expression. Additionally, we investigated the effect of siRNA transfection on these cells. Our findings indicate that OPN expression can be downregulated using OPN-specific siRNA in primary tumour and melanoma metastasis originated melanoma cell lines. We observed a reduction in cell proliferation and cell migration following effective silencing the OPN gene.

Since silencing a gene can influence the expression of various proteins, we utilized a Proteome Profiler Human XL Oncology Array to assess the expression levels of 84 cancer-related proteins. By comparing the expression patterns of the parental and transfected cell lines, we identified several proteins with differential expression. Notably, OPN protein expression exhibited a decrease in both OPN-silenced cell lines derived from primary tumours and metastases. Other proteins that displayed altered expression included EGFR, tenascin C, survivin, galectin-3 and enolase 2. Our research [76], as well as studies conducted by others [135] demonstrated significant reductions in the expression of OPN and the antiapoptotic protein survivin in association with BRAF inhibitor resistance. Survivin, an apoptosis inhibitor, is known to be associated with poor prognosis in cancers [136]. Moreover, recent findings by Chen and co-workers emphasized the crucial role of survivin in tumorigenesis [137]. The decreased protein expression of tenascin C and survivin in the OPN-siRNA transfected cell lines is highly consistent with the observed levels of OPN expression levels, which play crucial roles in various metastasis-associated mechanisms, including cell proliferation, apoptosis, invasion and migration [124]. Tenascin C expression has been established as vital for cellular invasion and migration and playing a key role in metastasis development [138]. Recent studies, have reported a significant correlation between OPN and EGFR expression in clear cell renal cell carcinoma [139]. Consistent with our findings, inhibition of OPN resulted in decreased EGFR expression and an increase in apoptotic cell death. Apoptosis was significantly enhanced in OPN knockout mice, concomitant with the downregulation of EGFR [140]. Additionally, we

observed that decreased OPN expression in the transfected primary tumour-derived cell line was associated with lower galectin-3 and enolase 2 protein levels. However, in the metastatic cell line, OPN silencing led to an increase in the expression of these proteins. Galectin-3 expression serves as both a marker and promoter of progression and metastasis in numerous tumours [141, 142]. Intriguingly, galectin-3 and OPN have been proposed as potential targets or predictors in future personalized anti-aging therapies [143]. Overexpression of galectin-3 and enolase 2 was detected in transfected metastatic cell lines, suggesting that both proteins play significant roles in promoting the aggressive phenotype of melanoma cells. The concurrent expression of these proteins and their contributions to tumour progression have not been previously reported in human malignant melanoma. Li et al. reported a substantial increase in the expression levels of galectin-3 and enolase 2, and other proteins associated with hepatocellular carcinoma progression [144]. Enolase 2 is a specific molecular marker used in cancer diagnosis, and has the ability to promote the migration and invasion of tumour cells by remodelling the actin cytoskeleton [145].

We hypothesize that the proteins affected in the OPN-siRNA silenced cells are involved in several biological processes. Galectin-3 and OPN are implicated in extracellular matrix binding, while EGFR, galectin-3, enolase 2, and survivin are involved in protein dimerization [18, 146-148]. Studies have demonstrated that down-regulation of galectin-3 and the other proteins is associated with decreased migration, invasion and reduced tumour growth [146, 149]. However, galectin-3 also plays a regulatory role in cancer stemness related pathways, including the EGFR/FGFR pathway. It has been reported that OPN induced migration and invasion are strongly linked to the activation of different EGF receptors [150]. Consequently, decreased level of OPN and other proteins may contribute to a less aggressive phenotype. Furthermore, three of the altered proteins (EGFR, OPN and tenascin C) are linked to the PI3K-Akt signaling pathway. Additionally, EGFR, galectin-3 and OPN potentially influence the extracellular

signal-regulated RAF/MEK/ERK pathway [151-154]. Both pathways are fundamental in melanoma tumorigenesis [155, 156]. EGFR, OPN and tenascin C also play crucial roles in the focal adhesion pathway.The silencing of multiprotein focal adhesion complexes by OPN-siRNA can affect the connection between the extracellular matrix and cytoskeleton, regulating cell proliferation, differentiation, and motility [157]. These pathways alterations are significantly importance in the pathogenesis of melanoma as they impact tumorigenesis, cellular growth, chemoresistance, invasion and migration [3, 158].

In summary, our findings demonstrate that the expression of OPN in melanoma cells serves a strong predictor of poor prognosis. Multivariate analysis confirmed the significant predictive value of OPN for primary melanoma patient survival. This study provides further evidence supporting the significance of OPN in the biology of melanoma. Moreover, we have shown that a high level of OPN expression is associated with a more aggressive phenotype in melanoma. Notably, our study is the first to reveal differences in protein expression between untreated melanoma cell lines and those transfected with OPN-siRNA. Our results suggest that silencing the OPN gene can promote the proliferation and invasion of melanoma cells by influencing the expression of EGFR, tenascin C, survivin, galectin-3 and enolase 2. Our findings highlight the potential of targeting OPN as a therapeutic strategy for melanoma.

In conclusion, we observed nuclear translocation of the NF-κβ p65 protein in a melanoma cell line with high OPN mRNA expression, indicating the activation the NF-κβ pathway activation by OPN. By employing siRNA to inhibit OPN expression in melanoma cell lines, we observed decreased cell proliferation and invasion *in vitro*. These results strongly suggest that OPN overexpression plays a significant role in melanoma progression and that successful inhibition of OPN expression can be achieved in melanoma cells. Therefore, targeting OPN overexpression holds promise as a potential therapeutic approach for melanoma.

Summary

Osteopontin (OPN), a multifunctional glycophosphoprotein, plays different roles during cancer progression. In addition, to multiple intra- and extracellular functions, it facilitates migration of tumour cells, has crucial role in cell adhesion and is associated with increased metastasis formation. In our previous gene expression studies the OPN showed the highest expression level in melanomas with poor clinical outcome. The aim of the present study was to validate our previous microarray data. We also investigated OPN expression, cellular localization and its relationship with NF-κβ protein levels in primary and metastatic melanoma cell lines by immunohistochemistry. Therefore, the purpose of this study was to further characterize the function of OPN in tumorigenesis using melanoma cell lines and siRNA-mediated knockdown of OPN.

We verified our results by qRT-PCR and immunhistochemistry on tissue microarray and observed that more than 50% of tissues showed high protein expression and was significantly associated with poor prognosis. We applied qRT-PCR to identify high levels of OPN expression in the majority of cell lines. Our *in vitro* experiments, nuclear translocation of the NF-κβ p65 protein was observed in a cell line with high OPN expression. siRNA-mediated OPN knockdown led to decreased OPN expression in melanoma cell lines, which was associated with decreased cell proliferation and invasion. Proteome Profiler Oncology Array was used to determine protein expression patterns of original and transfected cell lines pairs and we found significantly different protein expression.

In summary, we showed that a high expression level of OPN is associated with a more aggressive phenotype in melanoma. Our results revealed for the first time that silencing the OPN gene influences proliferation and invasion of melanoma cells by effecting EGFR, tenascin C, survivin, galectin-3 and enolase 2 expression. Taken together these data suggest that OPN might be an ideal target for drug development and therapies.

Összefoglalás

Az oszteopontin (OPN) egy olyan multifunkcionális glükofoszfoprotein, mely számos daganat progressziójában fontos szerepet játszik. Elősegítheti a daganatos sejtek migrációját, döntő szerepet játszik a sejtadhézióban és szoros összefüggést mutat a metasztázisok jelenlétével. Korábbi génexpressziós vizsgálataink szerint a rosszabb prognózisú melanomákban a legmagasabb expressziós szintet az OPN gén mutatta. Ezért célul tűztük ki az OPN daganat progresszióban betöltött szerepének tanulmányozását eltérő viselkedésű melanomák és különböző eredetű melanoma sejtvonalak segítségével. Vizsgáltuk az OPN molekulához kapcsolódó egyik fő szignalizációs útvonalban részt vevő NF-κβ p65 fehérje kifejeződését eltérő biológiai viselkedésű humán melanoma sejtvonalakon immunfluoreszcens jelölés segítségével.

A génexpressziós adataink jó korrelációt mutattak munkacsoportunk előzetes mRNS expressziós értékeivel. A fehérje kifejeződését a vizsgált primer melanomák 90%-ában kimutattuk. Klinikai adatokkal történt korrelációs analízisünk szerint a fokozódó OPN-expressziós szintek kedvezőtlenül befolyásolják a betegség kimenetelét. *In vitro* kísérleteinkben NF-κβ p65 fehérje sejtmagi lokalizációját figyeltük meg egy magas OPN szintet mutató sejtvonalban. Az *OPN* gén csendesítése során az mRNS szint csökkenését tapasztaltuk. Továbbá megfigyeltük, hogy a transzfektált sejtvonal invazív képessége csökkent az eredeti sejtvonalhoz képest. A fehérje expressziós vizsgálataink során a tanulmányozott fehérjék többségénél csökkent expressziót figyeltünk meg az OPN csendesített sejtvonalakban.

Megállapíthatjuk, hogy az OPN emelkedett szintje jelentősen hozzájárul a daganatsejtek progressziójához, a metasztázisképzéshez, ezért melanomákban is fontos biomarkernek tekinthető. A géncsendesítést követően az *OPN* mRNS szint mellett a fehérje expressziója, valamint a sejtek invazív képessége is csökkent, ezért feltételezhetjük, hogy az OPN fontos lehet a melanoma terápia optimalizálásában.

MAIN STATEMENTS AND RESULTS

The main purpose of the doctoral thesis was to deeper understand the role of OPN expression during melanoma progression.

Investigation of OPN expression at the mRNA level in different subtypes of primary melanoma tissues and melanoma metastases:

- mRNA expression analysis of OPN showed an increased OPN level in advanced stage melanomas, with ulcerated surface and greater thickness.
- We found a significant increase in OPN mRNA levels during melanoma progression.

Analysis of the OPN protein expression in primary melanomas:

- OPN protein expression was associated with Breslow thickness and metastasis formation.
- We revealed that metastasis formation is more characteristic on primary melanomas with higher Breslow thickness.
- We examined the association between OPN expression levels and survival and found that high OPN expression was significantly associated with reduced survival in melanoma patients.

Determination of OPN gene expression patterns in melanoma cell lines derived from primary and metastatic tissues:

- We observed that the relative OPN mRNA expression significantly higher in the cell lines with metastatic potential.
- Comparing the relative osteopontin expression with BRAF mutational status of cell lines, we found that OPN expression was significantly higher in BRAF mutant cells compared to wild-type BRAF cells.

Examining the effect of RNAi on selected cell lines which are characterized with high OPN expression:

- We successfully inhibited OPN mRNA and protein expression in the selected melanoma cell lines.
- We observed a reduction in cell proliferation and cell migration following effective silencing the OPN gene.

Protein array analysis of the parental and siRNA silenced melanoma cell line pairs:

- Our study is the first to reveal differences in protein expression between untreated melanoma cell lines and those transfected with OPN-siRNA.

In conclusion, we showed that a high expression level of OPN is associated with a more aggressive phenotype in melanoma. Our results revealed for the first time that silencing the OPN gene influences proliferation and invasion of melanoma cells by effecting EGFR, tenascin C, survivin, galectin-3 and enolase 2 expression. Taken together these data suggest that OPN might be an ideal target for drug development and therapies.

References

1. Krajewski, C., et al., *Predictors of quality of life in melanoma patients 4 years after diagnosis: Results of a nationwide cohort study in Germany.* J Psychosoc Oncol, 2018. **36**(6): p. 734-753.
2. Turner, N., O. Ware, and M. Bosenberg, *Genetics of metastasis: melanoma and other cancers.* Clin Exp Metastasis, 2018. **35**(5-6): p. 379-391.
3. Schadendorf, D., et al., *Melanoma.* Lancet, 2018. **392**(10151): p. 971-984.
4. Sung, H., et al., *Global Cancer Statistics 2020: GLOBOCAN Estimates of Incidence and Mortality Worldwide for 36 Cancers in 185 Countries.* CA Cancer J Clin, 2021. **71**(3): p. 209-249.
5. Saginala, K., et al., *Epidemiology of Melanoma.* Med Sci (Basel), 2021. **9**(4).
6. Raimondi, S., M. Suppa, and S. Gandini, *Melanoma Epidemiology and Sun Exposure.* Acta Derm Venereol, 2020. **100**(11): p. adv00136.
7. Volkovova, K., et al., *Associations between environmental factors and incidence of cutaneous melanoma. Review.* Environ Health, 2012. **11 Suppl 1**: p. S12.
8. Kunz, M., M. Dannemann, and J. Kelso, *High-throughput sequencing of the melanoma genome.* Exp Dermatol, 2013. **22**(1): p. 10-7.
9. Gerami, P., et al., *Development of a prognostic genetic signature to predict the metastatic risk associated with cutaneous melanoma.* Clin Cancer Res, 2015. **21**(1): p. 175-83.
10. Cirenajwis, H., et al., *Molecular stratification of metastatic melanoma using gene expression profiling: Prediction of survival outcome and benefit from molecular targeted therapy.* Oncotarget, 2015. **6**(14): p. 12297-309.
11. Malissen, N. and J.J. Grob, *Metastatic Melanoma: Recent Therapeutic Progress and Future Perspectives.* Drugs, 2018. **78**(12): p. 1197-1209.
12. Ferguson, P.M., et al., *Impact of genomics on the surgical management of melanoma.* Br J Surg, 2018. **105**(2): p. e31-e47.
13. Rastrelli, M., et al., *Melanoma m1: diagnosis and therapy.* In Vivo, 2014. **28**(3): p. 273-85.
14. Shtivelman, E., et al., *Pathways and therapeutic targets in melanoma.* Oncotarget, 2014. **5**(7): p. 1701-52.
15. Rakosy, Z., et al., *Integrative genomics identifies gene signature associated with melanoma ulceration.* PLoS One, 2013. **8**(1): p. e54958.
16. Zhao, H., et al., *The role of osteopontin in the progression of solid organ tumour.* Cell Death Dis, 2018. **9**(3): p. 356.
17. Bandopadhyay, M., et al., *Osteopontin as a therapeutic target for cancer.* Expert Opin Ther Targets, 2014. **18**(8): p. 883-95.
18. Icer, M.A. and M. Gezmen-Karadag, *The multiple functions and mechanisms of osteopontin.* Clin Biochem, 2018. **59**: p. 17-24.
19. Wei, R., J.P.C. Wong, and H.F. Kwok, *Osteopontin -- a promising biomarker for cancer therapy.* J Cancer, 2017. **8**(12): p. 2173-2183.
20. Weber, G.F., G.S. Lett, and N.C. Haubein, *Osteopontin is a marker for cancer aggressiveness and patient survival.* Br J Cancer, 2010. **103**(6): p. 861-9.
21. Wai, P.Y. and P.C. Kuo, *Osteopontin: regulation in tumor metastasis.* Cancer Metastasis Rev, 2008. **27**(1): p. 103-18.

22. Yin, M., et al., *Osteopontin promotes the invasive growth of melanoma cells by activating integrin alphavbeta3 and down-regulating tetraspanin CD9.* Am J Pathol, 2014. **184**(3): p. 842-58.
23. Elder, D.E., et al., *The 2018 World Health Organization Classification of Cutaneous, Mucosal, and Uveal Melanoma: Detailed Analysis of 9 Distinct Subtypes Defined by Their Evolutionary Pathway.* Arch Pathol Lab Med, 2020. **144**(4): p. 500-522.
24. Guo, W., H. Wang, and C. Li, *Signal pathways of melanoma and targeted therapy.* Signal Transduct Target Ther, 2021. **6**(1): p. 424.
25. Rossi, M., et al., *Familial Melanoma: Diagnostic and Management Implications.* Dermatol Pract Concept, 2019. **9**(1): p. 10-16.
26. Truderung, O.A., et al., *Melanoma susceptibility: an update on genetic and epigenetic findings.* Int J Mol Epidemiol Genet, 2021. **12**(5): p. 71-89.
27. Tagliabue, E., et al., *MC1R variants as melanoma risk factors independent of at-risk phenotypic characteristics: a pooled analysis from the M-SKIP project.* Cancer Manag Res, 2018. **10**: p. 1143-1154.
28. Black, J.O., *Xeroderma Pigmentosum.* Head Neck Pathol, 2016. **10**(2): p. 139-44.
29. Teixido, C., et al., *Molecular Markers and Targets in Melanoma.* Cells, 2021. **10**(9).
30. Paluncic, J., et al., *Roads to melanoma: Key pathways and emerging players in melanoma progression and oncogenic signaling.* Biochim Biophys Acta, 2016. **1863**(4): p. 770-84.
31. Gajos-Michniewicz, A. and M. Czyz, *WNT Signaling in Melanoma.* Int J Mol Sci, 2020. **21**(14).
32. Sun, L. and J. Arbesman, *Canonical Signaling Pathways in Melanoma.* Clin Plast Surg, 2021. **48**(4): p. 551-560.
33. Ding, L., et al., *Prognostic biomarkers of cutaneous melanoma.* Photodermatol Photoimmunol Photomed, 2022. **38**(5): p. 418-434.
34. Deacon, D.C., E.A. Smith, and R.L. Judson-Torres, *Molecular Biomarkers for Melanoma Screening, Diagnosis and Prognosis: Current State and Future Prospects.* Front Med (Lausanne), 2021. **8**: p. 642380.
35. Ordonez, N.G., *Value of melanocytic-associated immunohistochemical markers in the diagnosis of malignant melanoma: a review and update.* Hum Pathol, 2014. **45**(2): p. 191-205.
36. Sandru, A., et al., *Prognostic value of melanoma inhibitory activity protein in localized cutaneous malignant melanoma.* J Skin Cancer, 2014. **2014**: p. 843214.
37. Hugel, R., et al., *Serum levels of hepatocyte growth factor as a potential tumor marker in patients with malignant melanoma.* Melanoma Res, 2016. **26**(4): p. 354-60.
38. Kruckel, A., et al., *Eosinophil-cationic protein - a novel liquid prognostic biomarker in melanoma.* BMC Cancer, 2019. **19**(1): p. 207.
39. de Lecea, M.V., et al., *Indoleamine 2,3 dioxygenase as a prognostic and follow-up marker in melanoma. A comparative study with LDH and S100B.* J Eur Acad Dermatol Venereol, 2017. **31**(4): p. 636-642.
40. Timerman, D., et al., *Vitamin D deficiency is associated with a worse prognosis in metastatic melanoma.* Oncotarget, 2017. **8**(4): p. 6873-6882.
41. Palmer, S.R., et al., *Circulating serologic and molecular biomarkers in malignant melanoma.* Mayo Clin Proc, 2011. **86**(10): p. 981-90.
42. Galanzha, E.I., et al., *In vivo liquid biopsy using Cytophone platform for photoacoustic detection of circulating tumor cells in patients with melanoma.* Sci Transl Med, 2019. **11**(496).
43. Lee, J.H., et al., *Pre-operative ctDNA predicts survival in high-risk stage III cutaneous melanoma patients.* Ann Oncol, 2019. **30**(5): p. 815-822.

44. Valpione, S., et al., *Plasma total cell-free DNA (cfDNA) is a surrogate biomarker for tumour burden and a prognostic biomarker for survival in metastatic melanoma patients.* Eur J Cancer, 2018. **88**: p. 1-9.
45. Guo, S., et al., *Serum miR-16: A Potential Biomarker for Predicting Melanoma Prognosis.* J Invest Dermatol, 2016. **136**(5): p. 985-993.
46. Tengda, L., et al., *Serum exosomal microRNAs as potent circulating biomarkers for melanoma.* Melanoma Res, 2018. **28**(4): p. 295-303.
47. Huang, N., K.J. Lee, and M.S. Stark, *Current Trends in Circulating Biomarkers for Melanoma Detection.* Front Med (Lausanne), 2022. **9**: p. 873728.
48. Aya-Bonilla, C.A., et al., *Detection and prognostic role of heterogeneous populations of melanoma circulating tumour cells.* Br J Cancer, 2020. **122**(7): p. 1059-1067.
49. Thomas, N.E., et al., *DNA methylation profiles in primary cutaneous melanomas are associated with clinically significant pathologic features.* Pigment Cell Melanoma Res, 2014. **27**(6): p. 1097-105.
50. Ghafouri-Fard, S., M. Gholipour, and M. Taheri, *MicroRNA Signature in Melanoma: Biomarkers and Therapeutic Targets.* Front Oncol, 2021. **11**: p. 608987.
51. Hulstaert, E., et al., *Long non-coding RNAs in cutaneous melanoma: clinical perspectives.* Oncotarget, 2017. **8**(26): p. 43470-43480.
52. Wilmott, J.S., et al., *Expression of the class 1 histone deacetylases HDAC8 and 3 are associated with improved survival of patients with metastatic melanoma.* Mod Pathol, 2015. **28**(7): p. 884-94.
53. Strub, T., R. Ballotti, and C. Bertolotto, *The "ART" of Epigenetics in Melanoma: From histone "Alterations, to Resistance and Therapies".* Theranostics, 2020. **10**(4): p. 1777-1797.
54. Revythis, A., et al., *Unraveling the Wide Spectrum of Melanoma Biomarkers.* Diagnostics (Basel), 2021. **11**(8).
55. Brunner, G., et al., *A Prognostic Gene Signature Expressed in Primary Cutaneous Melanoma: Synergism With Conventional Staging.* JNCI Cancer Spectr, 2018. **2**(3): p. pky032.
56. Amaral, T.M.S., et al., *Clinical validation of a prognostic 11-gene expression profiling score in prospectively collected FFPE tissue of patients with AJCC v8 stage II cutaneous melanoma.* Eur J Cancer, 2020. **125**: p. 38-45.
57. Gerami, P., et al., *Gene expression profiling for molecular staging of cutaneous melanoma in patients undergoing sentinel lymph node biopsy.* J Am Acad Dermatol, 2015. **72**(5): p. 780-5 e3.
58. Gastman, B.R., et al., *Identification of patients at risk of metastasis using a prognostic 31-gene expression profile in subpopulations of melanoma patients with favorable outcomes by standard criteria.* J Am Acad Dermatol, 2019. **80**(1): p. 149-157 e4.
59. Hsueh, E.C., et al., *Long-Term Outcomes in a Multicenter, Prospective Cohort Evaluating the Prognostic 31-Gene Expression Profile for Cutaneous Melanoma.* JCO Precis Oncol, 2021. **5**.
60. Belter, B., C. Haase-Kohn, and J. Pietzsch, *Biomarkers in Malignant Melanoma: Recent Trends and Critical Perspective*, in *Cutaneous Melanoma: Etiology and Therapy*, W.H. Ward and J.M. Farma, Editors. 2017: Brisbane (AU).
61. Kiefer, M.C., D.M. Bauer, and P.J. Barr, *The cDNA and derived amino acid sequence for human osteopontin.* Nucleic Acids Res, 1989. **17**(8): p. 3306.
62. Bastos, A., et al., *The Intracellular and Secreted Sides of Osteopontin and Their Putative Physiopathological Roles.* Int J Mol Sci, 2023. **24**(3).
63. Moorman, H.R., et al., *Osteopontin: A Key Regulator of Tumor Progression and Immunomodulation.* Cancers (Basel), 2020. **12**(11).

64. Shevde, L.A. and R.S. Samant, *Role of osteopontin in the pathophysiology of cancer.* Matrix Biol, 2014. **37**: p. 131-41.
65. Hao, C., et al., *Human osteopontin: Potential clinical applications in cancer (Review).* Int J Mol Med, 2017. **39**(6): p. 1327-1337.
66. Ahmed, M., et al., *An Osteopontin/CD44 Axis in RhoGDI2-Mediated Metastasis Suppression.* Cancer Cell, 2016. **30**(3): p. 432-443.
67. Shirasaki, T., et al., *The osteopontin-CD44 axis in hepatic cancer stem cells regulates IFN signaling and HCV replication.* Sci Rep, 2018. **8**(1): p. 13143.
68. Zhang, H., et al., *Osteopontin knockdown inhibits alphav,beta3 integrin-induced cell migration and invasion and promotes apoptosis of breast cancer cells by inducing autophagy and inactivating the PI3K/Akt/mTOR pathway.* Cell Physiol Biochem, 2014. **33**(4): p. 991-1002.
69. Maeda, N., et al., *Osteopontin-integrin interaction as a novel molecular target for antibody-mediated immunotherapy in adult T-cell leukemia.* Retrovirology, 2015. **12**: p. 99.
70. Yu, X., et al., *Osteopontin promotes hepatocellular carcinoma progression via the PI3K/AKT/Twist signaling pathway.* Oncol Lett, 2018. **16**(4): p. 5299-5308.
71. Fan, C.S., et al., *Osteopontin-integrin engagement induces HIF-1alpha-TCF12-mediated endothelial-mesenchymal transition to exacerbate colorectal cancer.* Oncotarget, 2018. **9**(4): p. 4998-5015.
72. Cheng, Y., et al., *Osteopontin Promotes Colorectal Cancer Cell Invasion and the Stem Cell-Like Properties through the PI3K-AKT-GSK/3beta-beta/Catenin Pathway.* Med Sci Monit, 2019. **25**: p. 3014-3025.
73. Zhao, Y. and C. Huang, *The role of osteopontin in the development and metastasis of melanoma.* Melanoma Res, 2021. **31**(4): p. 283-289.
74. Haga, Y., et al., *Overexpression of c-Jun contributes to sorafenib resistance in human hepatoma cell lines.* PLoS One, 2017. **12**(3): p. e0174153.
75. Mirzaei, A., et al., *Osteopontin b and c isoforms: Molecular Candidates Associated with Leukemic Stem Cell Chemoresistance in Acute Myeloid Leukemia.* Asian Pac J Cancer Prev, 2017. **18**(6): p. 1707-1715.
76. Szasz, I., et al., *Molecular alterations associated with acquired resistance to BRAFV600E targeted therapy in melanoma cells.* Melanoma Res, 2019. **29**(4): p. 390-400.
77. Subraman, V., et al., *OPN -Revisited.* J Clin Diagn Res, 2015. **9**(6): p. ZE10-3.
78. Zhao, B., et al., *Osteopontin as a potential biomarker of proliferation and invasiveness for lung cancer.* J Cancer Res Clin Oncol, 2011. **137**(7): p. 1061-70.
79. Cho, W.Y., et al., *Suppression of tumor growth in lung cancer xenograft model mice by poly(sorbitol-co-PEI)-mediated delivery of osteopontin siRNA.* Eur J Pharm Biopharm, 2015. **94**: p. 450-62.
80. Tang, M., et al., *Effective delivery of osteopontin small interference RNA using exosomes suppresses liver fibrosis via TGF-beta1 signaling.* Front Pharmacol, 2022. **13**: p. 882243.
81. Nemoto, H., et al., *Osteopontin deficiency reduces experimental tumor cell metastasis to bone and soft tissues.* J Bone Miner Res, 2001. **16**(4): p. 652-9.
82. Ben-David-Naim, M., et al., *Targeted siRNA Nanoparticles for Mammary Carcinoma Therapy.* Cancers (Basel), 2019. **11**(4).
83. Larkin, J., et al., *Combined Nivolumab and Ipilimumab or Monotherapy in Untreated Melanoma.* N Engl J Med, 2015. **373**(1): p. 23-34.
84. Del Vecchio, M., et al., *The Pattern of Progression to First-Line Treatment with Dabrafenib and Trametinib in Patients with Unresectable or Metastatic, BRAF-*

Mutated, Cutaneous Melanoma: Results of the Observational T-WIN Study. Cancers (Basel), 2023. **15**(7).
85. Dimitriou, F., G.V. Long, and A.M. Menzies, *Novel adjuvant options for cutaneous melanoma.* Ann Oncol, 2021. **32**(7): p. 854-865.
86. Dana, H., et al., *Molecular Mechanisms and Biological Functions of siRNA.* Int J Biomed Sci, 2017. **13**(2): p. 48-57.
87. Bumcrot, D., et al., *RNAi therapeutics: a potential new class of pharmaceutical drugs.* Nat Chem Biol, 2006. **2**(12): p. 711-9.
88. Lam, J.K., et al., *siRNA Versus miRNA as Therapeutics for Gene Silencing.* Mol Ther Nucleic Acids, 2015. **4**(9): p. e252.
89. Mahmoodi Chalbatani, G., et al., *Small interfering RNAs (siRNAs) in cancer therapy: a nano-based approach.* Int J Nanomedicine, 2019. **14**: p. 3111-3128.
90. Weng, Y., et al., *RNAi therapeutic and its innovative biotechnological evolution.* Biotechnol Adv, 2019. **37**(5): p. 801-825.
91. Pengnam, S., et al., *Delivery of small interfering RNAs by nanovesicles for cancer therapy.* Drug Metab Pharmacokinet, 2022. **42**: p. 100425.
92. Tian, Z., et al., *Insight Into the Prospects for RNAi Therapy of Cancer.* Front Pharmacol, 2021. **12**: p. 644718.
93. Sasayama, Y., et al., *In vivo activation of PEGylated long circulating lipid nanoparticle to achieve efficient siRNA delivery and target gene knock down in solid tumors.* J Control Release, 2019. **311-312**: p. 245-256.
94. Li, L., et al., *Dual Tumor-Targeting Nanocarrier System for siRNA Delivery Based on pRNA and Modified Chitosan.* Mol Ther Nucleic Acids, 2017. **8**: p. 169-183.
95. Majumder, P., S. Bhunia, and A. Chaudhuri, *A lipid-based cell penetrating nano-assembly for RNAi-mediated anti-angiogenic cancer therapy.* Chem Commun (Camb), 2018. **54**(12): p. 1489-1492.
96. Sonoke, S., et al., *Tumor regression in mice by delivery of Bcl-2 small interfering RNA with pegylated cationic liposomes.* Cancer Res, 2008. **68**(21): p. 8843-51.
97. Katsurahara, K., et al., *ANO9 regulates PD-L2 expression and binding ability to PD-1 in gastric cancer.* Cancer Sci, 2021. **112**(3): p. 1026-1037.
98. Gershenwald, J.E. and R.A. Scolyer, *Melanoma Staging: American Joint Committee on Cancer (AJCC) 8th Edition and Beyond.* Ann Surg Oncol, 2018. **25**(8): p. 2105-2110.
99. Kiss, T., et al., *The role of osteopontin expression in melanoma progression.* Tumour Biol, 2015. **36**(10): p. 7841-7.
100. Kiss, T., et al., *Silencing Osteopontin Expression Inhibits Proliferation, Invasion and Induce Altered Protein Expression in Melanoma Cells.* Pathol Oncol Res, 2021. **27**: p. 581395.
101. Ladanyi, A., et al., *Sex-dependent liver metastasis of human melanoma lines in SCID mice.* Melanoma Res, 1995. **5**(2): p. 83-6.
102. Lazar, V., et al., *Characterization of candidate gene copy number alterations in the 11q13 region along with BRAF and NRAS mutations in human melanoma.* Mod Pathol, 2009. **22**(10): p. 1367-78.
103. Livak, K.J. and T.D. Schmittgen, *Analysis of relative gene expression data using real-time quantitative PCR and the 2(-Delta Delta C(T)) Method.* Methods, 2001. **25**(4): p. 402-8.
104. Koh, S.S., et al., *Molecular classification of melanomas and nevi using gene expression microarray signatures and formalin-fixed and paraffin-embedded tissue.* Mod Pathol, 2009. **22**(4): p. 538-46.

105. Lueking, A., et al., *Determination and validation of off-target activities of anti-CD44 variant 6 antibodies using protein biochips and tissue microarrays.* Biotechniques, 2008. **45**(4): p. Pi-v.
106. Koroknai, V., et al., *Genomic profiling of invasive melanoma cell lines by array comparative genomic hybridization.* Melanoma Res, 2016. **26**(2): p. 100-7.
107. Tuzmen, S., J. Kiefer, and S. Mousses, *Validation of short interfering RNA knockdowns by quantitative real-time PCR.* Methods Mol Biol, 2007. **353**: p. 177-203.
108. Caffrey, D.R., et al., *siRNA off-target effects can be reduced at concentrations that match their individual potency.* PLoS One, 2011. **6**(7): p. e21503.
109. Szklarczyk, D., et al., *STRING v11: protein-protein association networks with increased coverage, supporting functional discovery in genome-wide experimental datasets.* Nucleic Acids Res, 2019. **47**(D1): p. D607-D613.
110. Liu, Y., A. Beyer, and R. Aebersold, *On the Dependency of Cellular Protein Levels on mRNA Abundance.* Cell, 2016. **165**(3): p. 535-50.
111. Nicolet, B.P. and M.C. Wolkers, *The relationship of mRNA with protein expression in CD8+ T cells associates with gene class and gene characteristics.* PLoS One, 2022. **17**(10): p. e0276294.
112. Maier, T., M. Guell, and L. Serrano, *Correlation of mRNA and protein in complex biological samples.* FEBS Lett, 2009. **583**(24): p. 3966-73.
113. Han, X., et al., *Osteopontin as a biomarker for osteosarcoma therapy and prognosis.* Oncol Lett, 2019. **17**(3): p. 2592-2598.
114. Maier, T., et al., *Osteopontin expression in plasma of melanoma patients and in melanocytic tumours.* J Eur Acad Dermatol Venereol, 2012. **26**(9): p. 1084-91.
115. Karagiannis, P., M. Fittall, and S.N. Karagiannis, *Evaluating biomarkers in melanoma.* Front Oncol, 2014. **4**: p. 383.
116. Kang, Z., et al., *Identification of Transcriptional Heterogeneity and Construction of a Prognostic Model for Melanoma Based on Single-Cell and Bulk Transcriptome Analysis.* Front Cell Dev Biol, 2022. **10**: p. 874429.
117. Ng, M.F., J.L. Simmons, and G.M. Boyle, *Heterogeneity in Melanoma.* Cancers (Basel), 2022. **14**(12).
118. Karami Fath, M., et al., *Current understanding of epigenetics role in melanoma treatment and resistance.* Cancer Cell Int, 2022. **22**(1): p. 313.
119. Rangaswami, H., A. Bulbule, and G.C. Kundu, *Osteopontin: role in cell signaling and cancer progression.* Trends Cell Biol, 2006. **16**(2): p. 79-87.
120. Packer, L., et al., *Osteopontin is a downstream effector of the PI3-kinase pathway in melanomas that is inversely correlated with functional PTEN.* Carcinogenesis, 2006. **27**(9): p. 1778-86.
121. Pang, X., et al., *Osteopontin as a multifaceted driver of bone metastasis and drug resistance.* Pharmacol Res, 2019. **144**: p. 235-244.
122. Guarneri, C., et al., *NFkappaB inhibition is associated with OPN/MMP9 downregulation in cutaneous melanoma.* Oncol Rep, 2017. **37**(2): p. 737-746.
123. Matusan-Ilijas, K., et al., *Osteopontin expression correlates with nuclear factor-kappaB activation and apoptosis downregulation in clear cell renal cell carcinoma.* Pathol Res Pract, 2011. **207**(2): p. 104-10.
124. Liu, J., et al., *Osteopontin promotes the progression of gastric cancer through the NF-kappaB pathway regulated by the MAPK and PI3K.* Int J Oncol, 2014. **45**(1): p. 282-90.
125. Park, M.H. and J.T. Hong, *Roles of NF-kappaB in Cancer and Inflammatory Diseases and Their Therapeutic Approaches.* Cells, 2016. **5**(2).

126. Xia, Y., S. Shen, and I.M. Verma, *NF-kappaB, an active player in human cancers.* Cancer Immunol Res, 2014. **2**(9): p. 823-30.
127. Das, R., et al., *Osteopontin: it's role in regulation of cell motility and nuclear factor kappa B-mediated urokinase type plasminogen activator expression.* IUBMB Life, 2005. **57**(6): p. 441-7.
128. Mansoori, B., S. Sandoghchian Shotorbani, and B. Baradaran, *RNA interference and its role in cancer therapy.* Adv Pharm Bull, 2014. **4**(4): p. 313-21.
129. Maduri, S., *Applicability of RNA interference in cancer therapy: Current status.* Indian J Cancer, 2015. **52**(1): p. 11-21.
130. Elazar, V., et al., *Sustained delivery and efficacy of polymeric nanoparticles containing osteopontin and bone sialoprotein antisenses in rats with breast cancer bone metastasis.* Int J Cancer, 2010. **126**(7): p. 1749-60.
131. Reufsteck, C., et al., *Silencing of skeletal metastasis-associated genes impairs migration of breast cancer cells and reduces osteolytic bone lesions.* Clin Exp Metastasis, 2012. **29**(5): p. 441-56.
132. Wu, X.L., et al., *Osteopontin knockdown suppresses the growth and angiogenesis of colon cancer cells.* World J Gastroenterol, 2014. **20**(30): p. 10440-8.
133. Xu, S.T., et al., *Role of osteopontin in the regulation of human bladder cancer proliferation and migration in T24 cells.* Mol Med Rep, 2015. **11**(5): p. 3701-7.
134. Zhou, Y., et al., *Osteopontin expression correlates with melanoma invasion.* J Invest Dermatol, 2005. **124**(5): p. 1044-52.
135. Ji, Z., et al., *Vemurafenib synergizes with nutlin-3 to deplete survivin and suppresses melanoma viability and tumor growth.* Clin Cancer Res, 2013. **19**(16): p. 4383-91.
136. Dong, H., et al., *Survivin expression and serum levels in pancreatic cancer.* World J Surg Oncol, 2015. **13**: p. 189.
137. Chen, X., et al., *Survivin and Tumorigenesis: Molecular Mechanisms and Therapeutic Strategies.* J Cancer, 2016. **7**(3): p. 314-23.
138. Grahovac, J., D. Becker, and A. Wells, *Melanoma cell invasiveness is promoted at least in part by the epidermal growth factor-like repeats of tenascin-C.* J Invest Dermatol, 2013. **133**(1): p. 210-20.
139. Matusan-Ilijas, K., et al., *EGFR expression is linked to osteopontin and Nf-kappaB signaling in clear cell renal cell carcinoma.* Clin Transl Oncol, 2013. **15**(1): p. 65-71.
140. Lee, S.H., et al., *Suppression of osteopontin inhibits chemically induced hepatic carcinogenesis by induction of apoptosis in mice.* Oncotarget, 2016. **7**(52): p. 87219-87231.
141. Ahmed, H. and D.M. AlSadek, *Galectin-3 as a Potential Target to Prevent Cancer Metastasis.* Clin Med Insights Oncol, 2015. **9**: p. 113-21.
142. Li, Y.S., et al., *Roles of galectin-3 in metabolic disorders and tumor cell metabolism.* Int J Biol Macromol, 2020. **142**: p. 463-473.
143. Sanchis-Gomar, F., et al., *Galectin-3, osteopontin and successful aging.* Clin Chem Lab Med, 2016. **54**(5): p. 873-7.
144. Li, X., et al., *Novel role of semaphorin 3A in the growth and progression of hepatocellular carcinoma.* Oncol Rep, 2017. **37**(6): p. 3313-3320.
145. Vizin, T. and J. Kos, *Gamma-enolase: a well-known tumour marker, with a less-known role in cancer.* Radiol Oncol, 2015. **49**(3): p. 217-26.
146. Nangia-Makker, P., V. Hogan, and A. Raz, *Galectin-3 and cancer stemness.* Glycobiology, 2018. **28**(4): p. 172-181.
147. Lavoie, H., et al., *Dimerization-induced allostery in protein kinase regulation.* Trends Biochem Sci, 2014. **39**(10): p. 475-86.

148. Ibrahim, T.M., et al., *Small-Molecule Intervention At The Dimerization Interface Of Survivin By Novel Rigidized Scaffolds.* Drug Des Devel Ther, 2019. **13**: p. 4247-4263.
149. Yue, B., *Biology of the extracellular matrix: an overview*. J Glaucoma, 2014. **23**(8 Suppl 1): p. S20-3.
150. Tuck, A.B., et al., *Osteopontin-induced migration of human mammary epithelial cells involves activation of EGF receptor and multiple signal transduction pathways.* Oncogene, 2003. **22**(8): p. 1198-205.
151. Eberwein, P., et al., *Modulation of focal adhesion constituents and their down-stream events by EGF: On the cross-talk of integrins and growth factor receptors.* Biochim Biophys Acta, 2015. **1853**(10 Pt A): p. 2183-98.
152. Jones, P.L., J. Crack, and M. Rabinovitch, *Regulation of tenascin-C, a vascular smooth muscle cell survival factor that interacts with the alpha v beta 3 integrin to promote epidermal growth factor receptor phosphorylation and growth.* J Cell Biol, 1997. **139**(1): p. 279-93.
153. Hayashi, C., et al., *Serum osteopontin, an enhancer of tumor metastasis to bone, promotes B16 melanoma cell migration.* J Cell Biochem, 2007. **101**(4): p. 979-86.
154. Huang, R.H., et al., *Osteopontin Promotes Cell Migration and Invasion, and Inhibits Apoptosis and Autophagy in Colorectal Cancer by activating the p38 MAPK Signaling Pathway.* Cell Physiol Biochem, 2017. **41**(5): p. 1851-1864.
155. Eke, I. and N. Cordes, *Focal adhesion signaling and therapy resistance in cancer.* Semin Cancer Biol, 2015. **31**: p. 65-75.
156. Sun, Y., et al., *Signaling pathway of MAPK/ERK in cell proliferation, differentiation, migration, senescence and apoptosis.* J Recept Signal Transduct Res, 2015. **35**(6): p. 600-4.
157. Savoia, P., et al., *Targeting the ERK Signaling Pathway in Melanoma.* Int J Mol Sci, 2019. **20**(6).
158. Zhang, X.Y. and P.Y. Zhang, *Genetics and epigenetics of melanoma.* Oncol Lett, 2016. **12**(5): p. 3041-3044.

Publications

UNIVERSITY of DEBRECEN

UNIVERSITY AND NATIONAL LIBRARY
UNIVERSITY OF DEBRECEN
H-4002 Egyetem tér 1, Debrecen
Phone: +3652/410-443, email: publikaciok@lib.unideb.hu

Registry number: DEENK/17/2023.PL
Subject: PhD Publication List

Candidate: Tímea Kiss
Doctoral School: Doctoral School of Health Sciences
MTMT ID: 10048422

List of publications related to the dissertation

1. **Kiss, T.**, Jámbor, K., Koroknai, V., Szász, I., Bárdos, H., Mokánszki, A., Ádány, R., Balázs, M.: Silencing Osteopontin Expression Inhibits Proliferation, Invasion and Induce Altered Protein Expression in Melanoma Cells.
Pathol. Oncol. Res. 27, 1-10, 2021.
IF: 2.874

2. **Kiss, T.**, Ecsedi, S., Vízkeleti, L., Koroknai, V., Emri, G., Kovács, N., Ádány, R., Balázs, M.: The role of osteopontin expression in melanoma progression.
Tumor Biol. 36 (10), 7841-7847, 2015.
DOI: http://dx.doi.org/10.1007/s13277-015-3495-y
IF: 2.926

List of other publications

3. Szász, I., **Kiss, T.**, Mokánszki, A., Koroknai, V., Deák, J., Patel, V., Jámbor, K., Ádány, R., Balázs, M.: Identification of liquid biopsy-based mutations in colorectal cancer by targeted sequencing assays.
Mol. Cell. Probes. 67, 1-8, 2023.
DOI: http://dx.doi.org/10.1016/j.mcp.2022.101888
IF: 3.285 (2021)

4. Jámbor, K., Koroknai, V., **Kiss, T.**, Szász, I., Pikó, P., Balázs, M.: Gene Expression Patterns of Osteopontin Isoforms and Integrins in Malignant Melanoma.
Pathol. Oncol. Res. 28, 1-12, 2022.
DOI: http://dx.doi.org/10.3389/pore.2022.1610608
IF: 2.874 (2021)

DEBRECENI EGYETEM * Egyetemi és Nemzeti Könyvtár *

UNIVERSITY of DEBRECEN

UNIVERSITY AND NATIONAL LIBRARY
UNIVERSITY OF DEBRECEN
H-4002 Egyetem tér 1, Debrecen
Phone: +3652/410-443, email: publikaciok@lib.unideb.hu

5. Szász, I., Koroknai, V., Patel, V., Hajdú, T., **Kiss, T.**, Ádány, R., Balázs, M.: Cell Proliferation Is Strongly Associated with the Treatment Conditions of an ER Stress Inducer New Anti-Melanoma Drug in Melanoma Cell Lines.
Biomedicines. 9 (2), 1-19, 2021.
DOI: http://dx.doi.org/10.3390/biomedicines9020096
IF: 4.757

6. Patel, V., Szász, I., Koroknai, V., **Kiss, T.**, Balázs, M.: Molecular Alterations Associated with Acquired Drug Resistance during Combined Treatment with Encorafenib and Binimetinib in Melanoma Cell Lines.
Cancers (Basel). 13 (23), 1-22, 2021.
DOI: http://dx.doi.org/10.3390/cancers13236058
IF: 6.575

7. Szász, I., Koroknai, V., **Kiss, T.**, Vízkeleti, L., Ádány, R., Balázs, M.: Molecular alterations associated with acquired resistance to BRAFV600E targeted therapy in melanoma cells.
Melanoma Res. 29 (4), 390-400, 2019.
DOI: http://dx.doi.org/10.1097/CMR.0000000000000588
IF: 2.75

8. Vízkeleti, L., **Kiss, T.**, Koroknai, V., Ecsedi, S., Papp, O., Szász, I., Ádány, R., Balázs, M.: Altered integrin expression patterns revealed by microarray in human cutaneous melanoma.
Melanoma Res. 27 (3), 180-188, 2017.
IF: 3.135

9. Koroknai, V., Ecsedi, S., Vízkeleti, L., **Kiss, T.**, Szász, I., Lukács, A., Papp, O., Ádány, R., Balázs, M.: Genomic profiling of invasive melanoma cell lines by array comparative genomic hybridization.
Melanoma Res. 2, 100-107, 2016.
DOI: http://dx.doi.org/10.1097/CMR.0000000000000227
IF: 2.615

10. Ecsedi, S., Hernandez, V. H., Lima, S. C., Vízkeleti, L., Tóth, R., Lázár, V., Koroknai, V., **Kiss, T.**, Emri, G., Herceg, Z., Ádány, R., Balázs, M.: DNA methylation characteristics of primary melanomas with distinct biological behaviour.
PloS One. 9 (5), e96612, 2014.
DOI: http://dx.doi.org/10.1371/journal.pone.0096612
IF: 3.234

UNIVERSITY AND NATIONAL LIBRARY
UNIVERSITY OF DEBRECEN
H-4002 Egyetem tér 1, Debrecen
Phone: +3652/410-443, email: publikaciok@lib.unideb.hu

11. Vízkeleti, L., Ecsedi, S., Rákosy, Z., Orosz, A., Lázár, V., Emri, G., Koroknai, V., **Kiss, T.**, Ádány, R., Balázs, M.: The role of CCND1 alterations during the progression of cutaneous malignant melanoma.
Tumor Biol. 33 (6), 2189-2199, 2012.
DOI: http://dx.doi.org/10.1007/s13277-012-0480-6
IF: 2.518

Total IF of journals (all publications): 37,543
Total IF of journals (publications related to the dissertation): 5,8

The Candidate's publication data submitted to the iDEa Tudóstér have been validated by DEENK on the basis of the Journal Citation Report (Impact Factor) database.

17 January, 2023

DEBRECENI EGYETEM * Egyetemi és Nemzeti Könyvtár *

Keywords

malignant melanoma, osteopontin expression, tissue microarray, RNA interference, OPN knockdown, protein expression profile, invasion, proliferation

Kulcsszavak

malignus melanoma, oszteopontin expresszió, szöveti microarray, RNS interferencia, OPN géncsendesítés, fehérje expressziós profil, invázió, proliferáció

Acknowledgements

First and foremost, I wish to thank my supervisor Professor Margit Balázs, who has introduced me into the world of cancer research, and helped and guided my research during both my undergraduate and graduate research studies.

I would like to express my thankfulness to Professor Róza Ádány for making my work in this institute possible, as well as for all of her support during PhD study.

I am thankful for my colleagues Viktória Koroknai, István Szász for their always generous help and their critique during my experiments.

I would like to acknowledge my colleagues of the Department of Public Health and Epidemiology for their help during my experiments, especially to Györgyné Kovács for her assistance.

Finally, I would like to say special thanks to my family for their support and patient.

Financial supports

This research was supported by the Hungarian National Research Fund (OTKA K112327), the Hungarian Academy of Sciences (grant number 2011 TKI 473), TÁMOP-4.2.2/B-10/1-20100024 and TÁMOP-4.2.2.A-11/1/KONV-2012-0031 projects; the TÁMOP projects are co-financed by the European Union and the European Social Fund. This research was also supported by the European Union and the State of Hungary, co-financed by the European Social Fund in the framework of the TÁMOP-4.2.4.A/2-11/1-2012-0001 'National Excellence Program'. This research was also supported by the National Research Development and Innovation Fund (grant number K112327), by the European Regional Development Fund (GINOP-2.3.2-15-2016-00005), by the ÚNKP-19-3 New National Excellence Program of the Ministry for Innovation and Technology as well as by the Hungarian Academy of Sciences (MTA11010 and TK2016-78).

Appendix

Supplementary Table 1. Relative protein expression of 84 cancer-related proteins in melanoma cell lines

Sl. No.	Positions of the Proteins on the Array	Proteins Name	WM278	WM1617	WM278 OPN-siRNA	WM1617 OPN-siRNA
	A1/A2	**Reference spots**	100	100	100	100
1	A3/A4	**α-Fetoprotein**	0	8.7	0	15.86
2	A5/A6	**Amphiregulin**	0	0	0	4.18
3	A7/A8	**Angiopoietin-1**	9.98	0	0	4.07
4	A9/A10	**Angiopoietin-like 4**	0	8.2	0	17.06
5	A11/A12	**ENPP-2/Autotaxin**	0	5.14	0	18.91
6	A13/A14	**Axl**	21.18	0	0	0
7	A15/A16	**BCL-x**	0	6.21	0	0
8	A17/A18	**CA125/MUC16**	0	0	0	0
9	A19/A20	**E-Cadherin**	0	0	0	0
10	A21/A22	**VE-Cadherin**	0	18.57	0	10.46
11	B3/B4	**CapG**	0	56.15	0	43.29
12	B5/B6	**Carbonic Anhydrase IX**	0	11.97	0	10.52
13	B7/B8	**Cathepsin B**	9.76	25.34	0	18.23
14	B9/B10	**Cathepsin D**	11.03	21.97	0	27.24
15	B11/B12	**Cathepsin S**	40.39	9.4	27.27	14.65
16	B13/B14	**CEACAM-5**	0	0	0	6.1
17	B15/B16	**Decorin**	0	0	0	5.24
18	B17/B18	**Dkk-1**	0	0	0	0
19	B19/B20	**DLL1**	0	4.83	0	9.58
20	B21/B22	**EGFR/ErbB1**	32.34	25.8	14.19	12.42
21	C3/C4	**Endoglin/CD105**	22.89	33.53	23.22	45.6
22	C5/C6	**Endostatin**	0	0	0	0
23	C7/C8	**Enolase 2**	75.83	67.93	31.06	96.61
24	C9/C10	**eNOS**	0	0	0	4.37
25	C11/C12	**EpCAM/TROP1**	0	0	0	3.12
26	C13/C14	**ERα/NR3A1**	0	0	0	0
27	C15/C16	**ErbB2**	12.12	4.36	0	14.4
28	C17/C18	**ErbB3/Her3**	10.06	9.82	0	11.01
29	C19/C20	**ErbB4**	0	0	0	4.96
30	C21/C22	**FGF basic**	33.02	8.89	6.36	13.77
31	D1/D2	**FoxC2**	0	0	0	0
32	D3/D4	**FoxO1/FKHR**	0	43.33	0	30.05
33	D5/D6	**Galectin-3**	63.83	82.67	12.9	88.84
34	D7/D8	**GM-CSF**	0	0	0	3.55
35	D9/D10	**CG α/β (HCG)**	0	13	0	8.8
36	D11/D12	**HGF R/c-Met**	0	0	0	0
37	D13/D14	**HIF-1α**	4.2	59.92	0	56.06
38	D15/D16	**HNF-3β**		0	0	4.63
39	D17/D18	**HO-1/HMOX1**	9.15	45.2	5.51	47.36
40	D19/D20	**ICAM-1/CD54**	14.56	38.85	4.89	37.7
41	D21/D22	**IL-2 Rα**	0	0	0	0

42	D23/D24	**IL-6**	0	0	3.62	8.23
43	E1/E2	**CXCL8/IL-8**	34.09	0	46.58	0
44	E3/E4	**IL-18 BPa**	0	0	0	4.18
45	E5/E6	**Kallikrein 3/PSA**	0	0	0	4.81
46	E7/E8	**Kallikrein 5**	0	0	0	0
47	E9/E10	**Kallikrien 6**	0	0	0	0
48	E11/E12	**Leptin**	0	0	0	0
49	E13/E14	**Lumican**	0	0	0	0
50	E15/E16	**CCL2/MCP-1**	96.97	0	14.32	0
51	E17/E18	**CCL8/MCP-2**	0	0	0	5.03
52	E19/E20	**CCL7/MCP-3**	0	0	0	0
53	E21/E22	**M-CSF**	0	0	0	11.83
54	E23/E24	**Mesothelin**	0	0	0	9.56
55	F1/F2	**CCL3/MIP-1α**	0	0	0	0
56	F3/F4	**CCL20/MIP-3α**	0	0	0	3.63
57	F5/F6	**MMP-2**	0	0	0	3.77
58	F7/F8	**MMP-3**	0	0	5.13	10.13
59	F9/F10	**MMP-9**	0	0	0	0
60	F11/F12	**MSP/MST1**	0	0	0	4.06
61	F13/F14	**MUC-1**	0	0	0	4.26
62	F15/F16	**Nectin-4**	0	0	0	4.07
63	F17/F18	**Osteopontin (OPN)**	78.09	48.9	41.58	30.72
64	F19/F20	**p27/Kip1**	0	22.07	0	12.24
65	F21/F22	**p53**	15.15	89.85	10.87	57.03
66	F23/F24	**PDGF-AA**	12.67	0	0	6.78
67	G1/G2	**CD31/PECAM-1**	0	0	0	0
68	G3/G4	**Progesterone R/NR3C3**	0	0	0	0
69	G5/G6	**Progranulin**	23.81	44.49	11.17	34.95
70	G7/G8	**Prolactin**	0	0	0	7.37
71	G9/G10	**Prostasin/Prss8**	0	0	0	0
72	G11/G12	**E-Selectin/CD62E**	0	0	0	0
73	G13/G14	**Serpin B5/Maspin**	0	0	0	0
74	G15/G16	**Serpin E1/PAI-1**	0	0	0	5.94
75	G17/G18	**Snail**	27.51	37.31	16.16	33.77
76	G19/G20	**SPARC**	15.04	41.63	7.98	31.95
77	G21/G22	**Survivin**	33.94	90.78	0	49.76
78	G23/G24	**Tenascin C**	47.84	66.78	32.16	21.15
79	H1/H2	**Thrombospondin-1**	0	0	0	0
80	H3/H4	**Tie-2**	0	0	0	5.18
81	H5/H6	**u-Plasminogen Activator/Urokinase**	0	0	0	4.4
82	H7/H8	**VCAM-1/CD106**	0	0	0	3.7
83	H9/H10	**VEGF**	0	0	0	2.77
84	H11/H12	**Vimentin**	16.77	31.25	25.68	31.06